1521-0111/99/2/133–146$35.00
MOLECULAR PHARMACOLOGY

https://doi.org/10.1124/molpharm.120.000091
Mol Pharmacol 99:133–146, February 2021

$GABA_A$ Receptors Expressed in Oligodendrocytes Cultured from the Neonatal Rat Contain $\alpha3$ and $\gamma1$ Subunits and Present Differential Functional and Pharmacological Properties [S]

Rainald Pablo Ordaz, Edith Garay, Agenor Limon, Alberto Pérez-Samartín, María Victoria Sánchez-Gómez, Leticia Robles-Martínez, Abraham Cisneros-Mejorado, Carlos Matute, and Rogelio O. Arellano

Instituto de Neurobiología, Laboratorio de Neurofisiología Celular, Universidad Nacional Autónoma de México, Juriquilla, Querétaro, México (R.P.O., E.G., L.R.-M., A.C.-M., R.O.A.); Mitchell Center for Neurodegenerative Diseases, Department of Neurology, School of Medicine, University of Texas Medical Branch at Galveston, Galveston, Texas (A.L.); and Achucarro Basque Center for Neuroscience, CIBERNED and Departamento de Neurociencias, Universidad del País Vasco (UPV/EHU), Leioa, Spain (A.P.-S., M.V.S.-G., C.M.)

Received June 12, 2020; accepted November 5, 2020

ABSTRACT

Oligodendrocytes (OLs) express functional $GABA_A$ receptors ($GABA_A$Rs) that are activated by GABA released at synaptic contacts with axons or by ambient GABA in extrasynaptic domains. In both instances, the receptors' molecular identity has not been fully defined. Furthermore, data on their structural diversity in different brain regions and information on age-dependent changes in their molecular composition are scant. This lack of knowledge has delayed access to a better understanding of the role of GABAergic signaling between neurons and OLs. Here, we used functional, and pharmacological analyses, as well as gene and protein expression of $GABA_A$R subunits, to explore the subunit combination that could explain the receptor functional profile expressed in OLs from the neonate rat. We found that $GABA_A$R composed of $\alpha3\beta2\gamma1$ subunits mimicked the characteristics of the endogenous receptor when expressed heterologously in *Xenopus laevis* oocytes. Either $\alpha3$ or $\gamma1$ subunit silencing by small interfering RNA transfection changed the GABA-response characteristics in oligodendrocyte precursor cells, indicating their participation in the endogenous receptor conformation. Thus, $\alpha3$ subunit silencing shifted the mean EC_{50} for GABA from 75.1 to 46.6 μM, whereas $\gamma1$ silencing reduced the current amplitude response by 55%. We also observed that β-carbolines differentially enhance GABA responses in oligodendroglia as compared with those in neurons. These results contribute to defining the molecular and pharmacological properties of $GABA_A$Rs in OLs. Additionally, the identification of β-carbolines as selective enhancers of $GABA_A$Rs in OLs may help to study the role of GABAergic signaling during myelination.

SIGNIFICANCE STATEMENT

GABAergic signaling through $GABA_A$ receptors ($GABA_A$Rs) expressed in the oligodendroglial lineage contributes to the myelination control. Determining the molecular identity and the pharmacology of these receptors is essential to define their specific roles in myelination. Using $GABA_A$R subunit expression and silencing, we identified that the $GABA_A$R subunit combination $\alpha3\beta2\gamma1$ conforms the bulk of $GABA_A$Rs in oligodendrocytes from rat neonates. Furthermore, we found that these receptors have differential pharmacological properties that allow specific positive modulation by β-carbolines.

Introduction

Oligodendrocytes (OLs) and their progenitor cells (OPCs) are endowed with membrane receptors sensitive to γ-aminobutyric acid (GABA), a key neurotransmitter in the central nervous system, suggesting an important role in the communication between neurons and oligodendroglial cells. Correspondingly, specific GABAergic synaptic neuron-OPC contacts have been demonstrated in several brain regions (Lin and Bergles, 2004; Jabs et al., 2005; Kukley et al., 2008; Káradóttir et al., 2008; Tanaka et al., 2009; Orduz et al., 2015; Zonouzi et al., 2015). Volume transmission has also been proposed as an important element for axon-glial chemical communication (Vélez-Fort et al., 2010; Wake et al., 2015). The main electrical response in OLs to GABA corresponds to the activation of a pentameric receptor-channel type A [$GABA_A$ receptor ($GABA_A$R)], allowing the efflux of Cl^- ions, causing membrane depolarization and the subsequent opening of voltage-dependent Ca^{2+} channels (Gilbert et al., 1984; Hoppe and Kettenmann, 1989; Kirchhoff and Kettenmann, 1992). This GABA response in OLs ultimately increases the intracellular Ca^{2+} concentration, which

Some information reported herein was presented during a poster session by Rainald Pablo Ordaz, Edith Garay, Carlos Matute, and Rogelio O. Arellano at the "XIV European Meeting on Glial Cells in Health and Disease, GLIA 2019" on 2019 July 10–13.

This study was supported by grants from CONACYT-México [No. 252121] and PAPIIT UNAM-México [No. IN203519] to R.O.A.'s laboratory; National Institutes of Health National Institute of Aging [Grant R21-AG053740] and National Institute of Mental Health [Grant R21-MH113177] and the Amon G. Carter Foundation to A.L.; and CIBERNED [CB06/05/0076] and the Ministry of Economy and Competitiveness, Government of Spain [SAF2016-75292-R] and Basque Government [IT1203-19] to C.M.
https://doi.org/10.1124/molpharm.120.000091.
[S] This article has supplemental material available at molpharm.aspetjournals.org.

is involved in numerous phenomena, including the myelination process (Cesetti et al., 2012; Cheli et al., 2015, 2016; Wake et al., 2015; Pitman and Young, 2016; Baraban et al., 2018; Krasnow et al., 2018). GABA sensitivity seems to be regulated throughout the course of OL maturation, with the lowest sensitivity observed in myelinating OLs in adulthood. Thus, the GABA response is maximal during postnatal development, a stage in which the premyelinating OLs contact with axons and initiate the myelinating program. It has been shown that GABA sensitivity is regulated by contact between the OLs and the axon through a mechanism that involves the regulation of protein subunit synthesis (Arellano et al., 2016). Importantly, $GABA_A$Rs expressed in perinatal OLs and OPCs present distinctive characteristics comparable to those displayed in neurons and astrocytes (von Blankenfeld et al., 1991; Bronstein et al., 1998; Williamson et al., 1998; Arellano et al., 2016). Whether the $GABA_A$R expressed during postnatal development has a similar molecular composition to the $GABA_A$R expressed in OPCs at different ages or brain areas (especially in gray matter vs. white matter) remains unknown, given that the observed characteristics and molecular identity indicate diversity in composition (see, e.g., Vélez-Fort et al., 2012; Passlick et al., 2013; Balia et al., 2015).

It is fundamental to determine the $GABA_A$R identity expressed in OLs during development, as well as its specific pharmacology, since GABAergic signaling is a prospective target for therapeutic strategies against demyelinating illness (e.g., Zonouzi et al., 2015; Shaw et al., 2018, 2019; Cisneros-Mejorado et al., 2019; Serrano-Regal et al., 2019). We proposed that the main receptor type in OLs and OPCs, from the optic nerve of P12 rats and forebrain of newborn rats, respectively, comprises a combination of the $\alpha3$, $\beta2$ or $\beta3$, and $\gamma1$ or $\gamma3$ subunits (Arellano et al., 2016). This is based on the functional and pharmacological profile of the GABA response in OLs and supported by information presented by distinct groups about the expression of $GABA_A$R subunits in the oligodendroglial lineage. Accordingly, the most abundant mRNA expressed for α subunits is for $\alpha3$ and $\alpha2$ subunits, whereas $\gamma2$ and $\beta1$ subunit mRNA expression is absent or low in OPC preparations (Cahoy et al., 2008; Larson et al., 2016).

A characteristic that distinguishes the oligodendroglial receptor, with respect to neuronal $GABA_A$Rs, is a positive modulatory effect of β-carbolines such as N-butyl-β-carboline-3-carboxylate (β-CCB; Arellano et al., 2016; Cisneros-Mejorado et al., 2019).

In this exploratory work, oligodendroglial $GABA_A$R subunits were cloned and heterologously expressed in accordance with the studies cited above and on the analyses of publicly available RNA expression data sets in OPCs. Then, functional, and pharmacological analyses of six possible $GABA_A$R combinations were performed. Their characteristics were compared with those displayed by the endogenous oligodendroglial $GABA_A$R. Priority was given to analyzing the possible binding site for β-CCB. Data showed that $\alpha3\beta2\gamma1$ $GABA_A$R closely mimicked the characteristics expressed by the endogenous receptor in OLs, including positive modulation by β-CCB that did not involve its binding to classic sites for benzodiazepines (BZDs). Moreover, knocking down the expression of either $\alpha3$ or $\gamma1$ subunits using the small interfering RNA (siRNA) technique in vitro produced changes in the endogenous oligodendroglial GABA response, thus indicating that these subunits are involved in the receptor conformation. Finally, the effect of different β-carbolines, tested on both GABA responses from neurons and OLs, showed that many β-carbolines had a differential effect between these cell types, suggesting that they could be used to specifically enhance the $GABA_A$R response expressed in OLs.

Materials and Methods

Animal Handling. All experiments were performed by trained personnel and conducted in accordance with the *Guide for the Care and Use of Laboratory Animals* by the US National Institutes of Health. The animal protocols were approved by the Ethics Committees of the Instituto de Neurobiología at the Universidad Nacional Autónoma de México (UNAM) and the University of Basque Country (UPV/EHU). All possible efforts were made to comply with 3R standards and minimize animal suffering and the number of animals used.

RNA Sequencing Data Bases. Three data sets, derived from public domain resources as described below, were used for transcriptomic analysis (Fig. 1, A and B). Bulk RNA from mouse brain OPCs expressing platelet-derived growth factor receptor alpha ($PDGFR\alpha^+$), a marker of OL progenitors (http://www.brainrnaseq.org; Zhang et al., 2014) were provided by Steven Sloan, who can be reached via the same website. Single cell data sets from three different regions in adult mice (P21–P90) were downloaded from the Gene Expression Omnibus (GSE75330; Marques et al., 2016) and the Allen Institute website (https://celltypes.brain-map.org/rnaseq; Tasic et al., 2016). From the first data set, a total of 81 nuclei from cortex (S1), inferred as OPCs based on the cluster analysis reported previously, and 125 nuclei from the corpus callosum were used. From the last data set, a single cell analysis of the visual cortex (V1) in adult mice (P53–P59), thus normalized RNA sequencing (RNA-Seq) from 30 $NeuN^-$ nuclei, grouped in the OPC-$PDGFR\alpha^+$ cluster, were used in the analysis. Detailed demographic characteristics, as well as technical white papers for data processing and quality control, can be downloaded from the same site. Confirmatory analyses of enrichment of OPC markers and lack of neuronal markers were performed for all data sets. For data analysis, gene expression level in each data set was transformed to fractional contribution (FC) to the total pool of mRNA available to produce $GABA_A$Rs (Sequeira et al., 2019). Fractional contribution is defined as the percentage of expression level of each subunit gene over the sum of all 19 genes for $GABA_A$Rs subunits in each mouse/cell. The means of the FC for each gene in each single cell data set (corpus callosum, S1 and V1 brain cortex) were averaged to build Fig. 1, A and B.

Reverse Transcription Polymerase Chain Reaction, Cloning, and Site-Directed Mutagenesis of $GABA_A$R Subunits from OLs. To verify the expression of $GABA_A$R subunits, cDNA was synthetized from total RNA extracted from fresh isolated OLs derived from optic nerves of P12 rats (see below) and used in polymerase chain reaction (PCR) assays. PCR products were amplified with the following primers: $\alpha3$, forward: 5′-ACC ACA CAA ATG TGG CAC TTC-3′, reverse: 5′-AGT CAC TGC ATC TCC AAG CC-3′; $\beta2$, forward: 5′-ATG TGG AGA GTC CGG AAA AG-3′, reverse: 5′-TTT CAG TTG

ABBREVIATIONS: AUF, arbitrary unit(s) of fluorescence; BZD, benzodiazepine; β-CCB, N-butyl β-carboline-3-carboxylate; β-CCE, ethyl 9H-pyrido[3,4-b]indole-3-carboxylate; β-CHM, 3-(hydroxymethyl)-β-carboline; D-R, dose-response; DIV, day(s) in vitro; DMCM, 4-ethyl-6,7-dimethoxy-9H-pyrido[3,4-b]indole-3-carboxylic acid methyl ester; DZP, diazepam; FC, fractional contribution; FMZ, flumazenil; $GABA_A$R, $GABA_A$ receptor; MBP, myelin basic protein; NR, normal Ringer's; OL, oligodendrocyte; OPC, oligodendrocyte precursor cell; PCR, polymerase chain reaction; PDGFRα, platelet-derived growth factor receptor-α; ROI, region of interest; RNA-Seq, RNA sequencing; siRNA, small interfering RNA.

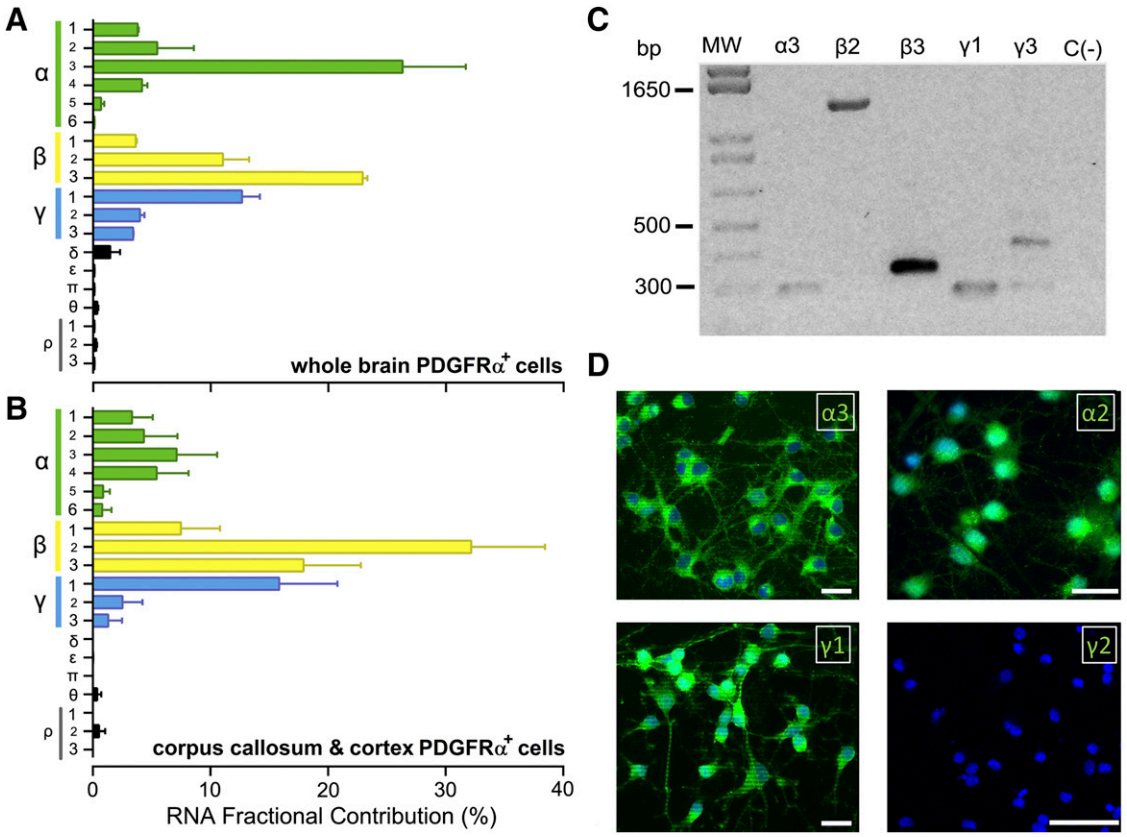

Fig. 1. Diversity of GABA$_A$R subunit expression in murine OPCs and OLs. (A) mRNA expression level for the 19 known GABA$_A$R subunit genes analyzed in PDGFRα^+ cells isolated by fluorescence-activated cell sorting from mice brains and assessed by RNA-Seq. The expression level of each GABA$_A$R subunit is represented as its FC to the total pool of RNA available to produce GABA$_A$R subunits. Data were obtained from http://www.brainrnaseq.org. (B) GABA$_A$R subunit RNA expression analysis from PDGFRα^+ cells from cortex (S1 and V1) and corpus callosum of adult mice. The expression level is represented as its FC to all RNA GABA$_A$R subunits available like in (A). Data were obtained from Gene Expression Omnibus (GSE75330) and https://celltypes.brain-map.org/rnaseq. (C) The gel shows amplification by reverse transcription (RT) PCR of GABA$_A$R subunit sequences expressed in purified OLs from rat P12 optic nerve. The expected product lengths are 266, 1311, 354, 231, and 404 and corresponded to α3, β2, β3, γ1, and γ3 subunits, respectively. bp, base pairs; MW, molecular weight marker; C(−), reaction negative control. (D) Analysis by immunocytochemistry of forebrain OPCs maintained in culture. Panels show images of the fluorescence signal for a specific antibody against the GABA$_A$R subunit proteins (in green) as indicated in each panel, and nuclei labeling with 4′,6-diamidino-2-phenylindole dihydrochloride (blue). Bars = 50 μm.

GGA GGC ACG TC -3′; β3, forward: 5′-CAC CCT GAT GGA ACA GTG CT-3′, reverse: 5′-ATG AGA GGA TTG TGA TCA TGA TTG-3′; γ1, forward: 5′-TAG GCG TGA GAC CCA CAG TA-3′, reverse: 5′-GCG ATT GGG CGT TGT TAT CC-3′; γ3, forward: 5′-ACC ATC AAT GCA GAG TGC CA-3′, and reverse: 5′-GCT GAG TGT GGT CAT GGT TA-3′. Glyceraldehyde-3-phosphate dehydrogenase amplification was used as a control with the oligonucleotide glyceraldehyde-3-phosphate dehydrogenase, forward, 5′-TCC CTC AAG ATT GTC AGC AA-3′, and reverse, 5′-AGA TCC ACA ACG GAT ACA TT-3′. The PCR conditions were an initial denaturation at 98°C for 30 seconds followed by 35 cycles at 98°C for 10 seconds, 55–60°C for 20 seconds, 72°C for 1 minute, and finally 72°C for 5 minutes using Phusion DNA Polymerase (Thermo Fisher Scientific, Waltham, MA). The complete coding sequences for α3, β2, β3, γ1, γ2, and γ3 subunits were amplified using the following primers: α3, forward: 5′-ATG ATA ACC ACA CAA ATG TGG C-3′, reverse: 5′-CTA CTG TTT GCG GAT CAT G-3′; β2, forward: 5′-ATG TGG AGA GTC CGG AAA-3′, reverse: 5′-TTA GTT CAC ATA GTA AAG CCA AT-3′; β3, forward: 5′-ATG TGG GGC TTT GCG GGA-3′, reverse: 5′-TCA GTT AAC ATA GTA CAG CCA GT-3′; γ1, forward: 5′-ATG GGT TCT GGG AAA GTC-3′, reverse: 5′-TTA TAA GTA TAG ATA TCC AAC CCA-3′; γ2, forward: 5′-ATG GCT GCA AAG CTG CTG-3′, and reverse: 5′-TTA AAG ATA TAG GTA TCC AAC CC-3′; γ3, forward: 5′-ATG GCT GCA AAG CTG CTG-3′, and reverse: 5′-TTA AAG ATA TAG GTA TCC AAC CC-3′. The PCR conditions were an initial denaturation at 98°C for 30 seconds followed by 35 cycles at 98°C for 10 seconds, 55–60°C for 20 seconds, 72°C for 70 seconds, and finally 72°C for 5 minutes. Each fragment obtained was cloned into pXENEX1 vector at the NcoI, BamHI, and NotI sites (e.g., Pérez-Samartín et al., 2017).

These plasmids were used as templates to make the site-directed mutagenesis of GABA$_A$R subunits using the following primers: α3(H126R), forward: 5′-GGA CTC CAG ATA CCT TCT TCA GAA ACG G-3′, reverse: 5′-GTG AGC CAC TGA TTT TTT ACC GTT TCT GAA G-3′; α3(S294I), forward: 5′-GTT CTC ACC ATG ACC ACC TTG ATC ATC AG-3′, reverse: 5′-GGT AAA GAG TTT CTG GCA CTG ATG ATC AAG G-3′; β2(N264I), forward: 5′-CCT GAC GAT GAC CAC AAT CAT CAC CC-3′, reverse: 5′-GAG TCT CCC GGA GAT GGG TGA TGA TT-3′; γ1(S282I), forward: 5′-CGG TTT TGA CTA TGA CAA CCC TCA TCA CA-3′, reverse: 5′-GAA ACC TTA GGT AAA GAT TTT CTA GCG ATT GTG ATG AG-3′, and the Pfu polymerase (Thermo Fisher Scientific). Plasmids were linearized with the Hind III enzyme and used as templates for in vitro synthesis using the T7 mMESSAGE mMACHINE kit following the standard protocol (Ambion; Invitrogen, Grand Island, NY). cRNAs were used for heterologous expression in *Xenopus laevis* oocytes.

Heterologous Functional Expression of GABA$_A$R Subunits in *Xenopus* Oocytes. Ovarian follicles of *X. laevis* were dissected by surgery as described previously (Arellano and Miledi, 1993). Briefly, female *X. laevis* frogs were obtained from Xenopus I (Ann Arbor, MI). The ovarian lobules were surgically removed under sterile conditions from anesthetized frogs using 0.1% aminobenzoic acid ethyl ester (Sigma-Aldrich Co., St. Louis, MO) and rendered hypothermic. After

surgery, frogs were sutured and allowed to recover from anesthesia. Frogs were maintained for 3–7 days in individual tanks until healing was complete and then housed in larger groups. No further oocytes were taken from them for at least 2 months. The follicles in stage VI (Dumont, 1972) were dissected from the lobules and maintained in normal Barth's solution (containing in millimolar: 88 NaCl, 1 KCl, 2.4 $NaHCO_3$, 0.33 $Ca(NO_3)_2$, 0.41 $CaCl_2$, 0.82 $MgSO_4$, 5 HEPES, adjusted to pH 7.4, and supplemented with 70 μg/ml gentamicin). Healthy isolated follicles were then injected with 50 nL of solution containing a mix of 2 or 3 (i.e., $\alpha3\beta2$, $\alpha3\beta3$, $\alpha3\beta2\gamma1$, $\alpha3\beta2\gamma3$, $\alpha3\beta3\gamma1$, $\alpha3\beta3\gamma3$, and $\alpha3\beta2\gamma2$; in proportion 1:1 or 1:1:1) of the cloned $GABA_AR$ subunit cRNA sequences (5 ng per follicle) or with 50 nL H_2O as a control, and cells were incubated at 18°C in normal Barth's solution. Then, 24 hours postinjection, follicles were treated with 0.5 mg/ml collagenase type 1 A (Sigma-Aldrich Co.) in normal Ringer's (NR) solution (containing, in millimolar, 115 NaCl, 5 KCl, 1.8 $CaCl_2$, and 5 HEPES; pH 7.0) for 30 minutes at room temperature. Cells were then washed several times with NR solution, and the oocytes were defolliculated using fine forceps under a stereomicroscope. Oocytes were incubated at 18°C in Barth's solution and monitored for their response to GABA and other drugs 3–6 days after cRNA injection. The electrical recording was made using the two-electrode voltage-clamp technique (Arellano and Miledi, 1993). For this, borosilicate glass micropipettes (filled with 3 M KCl) with a resistance of 1–2 MΩ were used. Currents were monitored using an Axon GenClamp 500B (Molecular Devices, San José, CA) amplifier, and signals were digitized and stored for further analysis using an analog-to-digital converter (Axon DigiData 1200; Molecular Devices) and specialized software (pClamp version 9; Molecular Devices). For electrical recordings, the oocytes were continuously superfused (10 ml/min) at room temperature with NR solution (unless otherwise stated), voltage-clamped at −60 mV and applied periodic voltage steps to −40 mV (1 second) every 40 seconds during the recording to monitor membrane conductance. All experimental groups were replicated using oocytes from at least three different frogs.

GABA and $GABA_AR$ allosteric modulators were applied through the superfusion solution to test their effects on oocytes expressing the different $GABA_AR$ subunit combinations. Dose-response curves were fitted to the following equation:

$$I/I_{max} = \left[(A1–A2)/1 + ([GABA]/EC_{50})^{nH}\right] + A2,$$

by the method of nonlinear least-squares fitting, where EC_{50} is the half-maximal effective concentration for GABA, nH is the slope factor (Hill coefficient), A1 and A2 are the initial and final normalized current (I) values, respectively, and [GABA] is the concentration of the neurotransmitter. For the inhibitory effect generated by Zn^{2+} administration was calculated the half-maximal inhibitory concentration (IC_{50}) fitting dose-response (D-R) curves for Zn^{2+} with the same equation and method.

Forebrain OPCs, Optic Nerve OLs, and Neuronal Cell Culture. Primary mixed glial cultures were prepared from newborn (P0–P2, of either sex) Sprague-Dawley rats as previously described (Arellano et al., 2016; Sánchez-Gómez et al., 2018). Briefly, forebrains were removed from the skulls, and cortices were isolated and digested by incubation (15 minutes, 37°C) in Hank's balanced salt solution containing 2.5% trypsin and 0.4% DNAse. The cells were dissociated by passage through needles (21G and 23G), centrifuged, and resuspended in Iscove's modified Dulbecco's medium supplemented with 10% FBS (Hyclone; Thermo Fisher Scientific) and antibiotic/antimycotic solution (Sigma-Aldrich Co.). Cells were seeded into poly-D-lysine–coated (10 μg/ml) 75 cm^2 flasks and maintained in culture at 37°C and 5% CO_2. After 10–15 days in culture, the flasks were shaken (400 rpm, 2 hours, 37°C) to remove loosely adherent microglia. The remaining OPCs on top of the confluent monolayer of astrocytes were dislodged by shaking overnight at 400 rpm. The cell suspension was then filtered through a 10 μm nylon mesh and plated on bacterial grade Petri dishes for 2 hours. The nonadherent OPCs that remained in suspension were recovered and plated again on bacterial grade Petri dishes for 1 hour. The resulting enriched forebrain OPC cell suspension was centrifuged and resuspended in a chemically defined medium (OPC medium) consisting of Dulbecco's modified Eagle's medium supplemented with 100 μg/ml transferrin, 60 ng/ml progesterone, 40 ng/ml sodium selenite, 5 μg/ml insulin, 16 μg/ml putrescine, and 100 μg/ml bovine serum albumin. Cells were plated onto poly-D-lysine–coated 12-mm-diameter coverslips in 24-well culture dishes at a density of 5×10^3 cells per well and cultured in the presence of the mitogenic factors platelet-derived growth factor-AA (5 ng/ml) and basic fibroblast growth factor (5 ng/ml) to expand their number and prevent their differentiation (here called proliferative medium). The purity of oligodendroglial cultures was confirmed by immunostaining with the antibodies against the oligodendroglial markers PDGFRα, Olig2, and NG2 that labeled more than 80% of cells, indicating that these cultures contained mostly OPCs at this stage.

In addition to cortical OPC purification, primary cultures of OLs derived from optic nerves of 12-day-old Sprague Dawley rats of either sex were obtained as described previously (Arellano et al., 2016). Cells were seeded on 24-well plates bearing 12-mm-diameter coverslips coated with poly-D-lysine (10 μg/ml) at a density of 10^4 cells per well. Cells were maintained at 37°C and 5% CO_2 in the differentiation medium. After 1 to 2 days in vitro, at least 97% of the cells were positive for the O4 antigen.

Primary cultures of cortical neurons were established according to a modified procedure (Larm et al., 1996). Briefly, cortical lobes of Wistar rat embryos (E18, of either sex) were isolated and digested in Hank's balanced salt solution (Gibco; Thermo Scientific) containing 0.25% trypsin and 0.4% DNAse. After, the tissues were dissociated with needles (21G, 23G, 25G) and centrifuged. The neurons were resuspended in B27 neurobasal medium (Gibco Thermo Scientific) supplemented with 10% FBS (Hyclone; Thermo Fisher Scientific) and seeded at 10^5 cells per well onto poly-L-ornithine–coated (30 μg/ml) 24-well plates bearing coverslips with a 12-mm diameter. The medium was replaced by serum-free B27-supplemented neurobasal medium (with antibiotic-antimycotic and 2 mM glutamine) 24 hours later. Cultures were maintained at 37°C and 5% CO_2. Rats were provided by the vivarium facilities either at the Instituto de Neurobiología at the Universidad Nacional Autónoma de México (UNAM) or at the University of Basque Country (UPV/EHU).

Whole-Cell Patch-Clamp. For the recording of membrane currents, cells [OPCs 1–4 days in vitro (DIV), OLs 1 DIV, or neurons 12–14 DIV] plated on coverslips were transferred to a recording chamber attached to a conventional inverted microscope (IX71; Olympus, Tokyo, Japan). They were continuously superfused and maintained at room temperature (22–25°C). The standard external solution (Attali et al., 1997; Pérez-Samartín et al., 2017) contained (in millimolar) 140 NaCl, 5.4 KCl, 2 $CaCl_2$, 1 $MgCl_2$, and 10 (4)-(2-hydroxyethyl)piperazine-1-ethanesulfonic acid (HEPES), and it was adjusted to pH 7.3 with NaOH. Electrophysiological recording was performed using either a MultiClamp 700B or an Axopatch 200B amplifier (Molecular Devices) to establish the standard whole-cell configuration. Patch-clamp pipettes (3–5 MΩ) were filled with internal solution (Pérez-Samartín et al., 2017) containing (in millimolar) 140 KCl, 2 $CaCl_2$, 2 $MgCl_2$, 10 HEPES, 11 EGTA, 2 Na-ATP, and 0.2 GTP, adjusted to pH 7.3 with KOH. Currents were recorded at a holding membrane potential of −80 mV, digitized with an analog-to-digital converter (DigiData 1440; Molecular Devices), and visualized and analyzed with specialized software (pClamp v10; Molecular Devices). In most cases, peak GABA current responses generated at −80 mV by drug superfusion were used for the analysis. Agonists and other drugs were added to the external solution from stock solutions, when necessary (e.g., for β-carboline application). DMSO was no more than 0.1% in the final solution.

Immunocytochemistry. To characterize primary cultures of OPCs and OLs, cells were immunoassayed with antibodies against oligodendroglial cell-specific markers: mouse anti-O4 (10 μg/ml; ref. MAB345; Millipore, Burlington, MA), mouse anti-PDGFRα (C-9)

(1:200; ref. sc-398206; Santa Cruz Biotechnology, Dallas, TX), rabbit anti-NG2 (1:300; ref. AB5320; Millipore), and rabbit anti-Olig2 (1:500; ref. AB9610; Millipore); to detect myelin expression, the mouse anti–myelin basic protein (MBP) was used (1:1000; ref. SMI-99; Covance, Princeton, NJ); astrocytes were identified by mouse anti–glial fibrillary acidic protein (2E1) (1:200; ref. sc-33673; Santa Cruz Biotechnology). For α2, α3, γ1, and γ2 subunit immunostaining, cells were treated with the corresponding antibody (anti-GABA$_A\alpha$2 1:100, ref. AGA002; anti-GABA$_A\alpha$3 1:100, ref. AGA003; and anti-GABA$_A\gamma$1 1:100, ref. AGA016; anti-GABA$_A\gamma$2 1:100, ref. AGA005; from Alomone Laboratories, Jerusalem, Israel). In all cases, cells were fixed in 4% paraformaldehyde in PBS for 30 minutes at room temperature. The fixed cultures were permeabilized with 0.1% Tween-20, blocked with 5% goat serum in PBS for 30 minutes, and incubated overnight at 4°C with the antibodies diluted in PBS containing 5% goat serum and 0.1% Tween-20. Then, cells were rinsed and incubated for 2 hours at room temperature with 1:200 goat anti-mouse IgG (H + L) conjugated with fluorescein isothiocyanate (ref. 81-6511; Invitrogen) or 1:200 goat anti-rabbit IgG (H + L) conjugated with Alexa Fluor 514 (ref. A-31558; Thermo Fisher Scientific) according to the host species of the primary antibodies. After five washes with PBS, samples were stained with 4 μg/ml 4′,6-diamidino-2-phenylindole dihydrochloride (Molecular Probes, Eugene, OR) to identify cell nuclei. In all cases, the absence of nonspecific interactions of secondary antibodies was corroborated by omitting the primary antibodies. Finally, the samples were mounted on VectaShield (Vector Laboratories, Burlingame, CA), and the preparations were visualized under an LSM510 laser scanning confocal microscope or under an Apotome optical sectioning fluorescence microscope (both from Zeiss, Oberkochen, Germany).

GABA$_A$R Subunit Silencing by siRNA Transfection. To reduce the expression of either α3 or γ1 subunit in cultured OPCs, the interference technique using siRNAs was used. These siRNAs were commercially designed (Dharmacon Inc., Lafayette, CO) for α3 (siGENOME Rat Gabra3 [24947] siRNA-SMARTpool) and γ1 (siGENOME Rat Gabrg1 [140674] siRNA-SMARTpool) using the target sequences NM_017069.3 and NM_080586.1, respectively. OPCs were seeded at a density of 4×10^4 cells per well in 24-well plates and allowed to attach overnight. Then, 1 DIV cells were transfected with 270 ng per well of α3-siRNA or γ1-siRNA using Lipofectamine 3000 (Invitrogen) following the manufacturer's instructions. For the control group (Control), cells were transfected in the same condition with the ON-TARGETplus Non-targeting Pool (SO-2686908G; Dharmacon Inc.). After 48–72 hours of transfection, siRNA-treated OPCs maintained in culture were used for immunocytochemistry using the methods described above or for electrophysiological monitoring. The arbitrary units of fluorescence (AUF) were estimated as optical density using ImageJ software (version 1.52i). Briefly, applying blind analysis the intensity of green was obtained from five regions of interest (ROIs) in every OPC preparation. AUF was calculated by normalizing the intensity values from each ROI against the background intensity value from each preparation, applying the following relationship: (intensity of the background – mean intensity of green measured in the ROIs)/intensity of the background (Cisneros-Mejorado et al., 2019). Then, for α3-siRNA and γ1-siRNA transfected OPCs and their corresponding control groups, the AUFs were normalized against the respective untreated groups. The GABA response elicited in transfected OPCs with either α3-siRNA or γ1-siRNA were compared with those of the corresponding control groups; OPCs were identified in the culture by their typical bipolar morphology and their rectifying current-voltage relationship, as well as the basic characteristics of the GABA response such as its low sensitivity to GABA, inhibition by Zn^{2+}, and/or enhancement by β-CCB (see Supplemental Fig. 2 and 3).

Substances. 7-Chloro-1-methyl-5-phenyl-3H-1,4-benzodiazepin-2(1H)-one [diazepam (DZP)]; 4-ethyl-6,7-dimethoxy-9H-pyrido[3,4-b] indole-3-carboxylic acid methyl ester (DMCM); β-CCB; β-carboline-3-carboxylic acid N-methylamide; ethyl 9H-pyrido[3,4-b]indole-3-carboxylate (β-CCE); 3-(hydroxymethyl)-β-carboline (β-CHM); tert-butyl β-carboline-3-carboxylate; N-methyl-N-[3-[3-[2-thienylcarbonyl]pyrazolo[1,5-a]pyrimidin-7-yl]phenyl]acetamide (indiplon); and 8-fluoro-5,6-dihydro-5-methyl-6-oxo-4H-imidazo[1,5-a][1,4]benzodiazepine-3-carboxylic acid, ethyl ester [flumazenil (FMZ)] were all obtained from Tocris Bioscience (Bristol, United Kingdom). Salts, DMSO, GABA, and ATP were from Sigma-Aldrich Co.

Statistical Analysis. All data were analyzed using p-CLAMP (version 10.6; Molecular Devices), R (version 3.2.3) with RStudio (Free Software Foundation Inc., Boston, MA), and GraphPad Prism (version 6.00; La Jolla, CA). Results are presented as means ± S.D., regularly; the sample size and the number of experiments were adjusted after initial data collection, and the final figures are indicated in each figure or the text. The statistical significance of differences between two data sets was tested with an unpaired two-tailed Student's t test. For multiple comparisons, a one-way ANOVA (Tukey's post hoc test) was used. The study was exploratory in nature and did not test a prespecified null hypothesis. The outcomes of the statistical tests cannot be interpreted as hypothesis testing but only as descriptive; thus, the indicated P values are therefore descriptive.

Results

Cloning and Expression of GABA$_A$R Subunits in OLs. To explore probable stoichiometries of GABA$_A$Rs expressed in OPCs, we examined the expression of all 19 genes for GABA$_A$R subunits in cells isolated by fluorescence-activated cell sorting, measured in bulk (bulk RNA-Seq) or individually (single cell RNA-Seq), from the cortex and corpus callosum, and deposited in public repositories (Zhang et al., 2014; Marques et al., 2016; Tasic et al., 2016). Only cells that were positive to PDGFRα^+, or clustered within the PDGFRα^+ category, were used for this analysis. The FC (Sequeira et al., 2019) of each subunit to the total pool of mRNAs available to conform GABA$_A$Rs was analyzed in each data set; results are illustrated in Figs. 1, A and B. In bulk RNA-Seq, α3 was the main expressed subunit, followed by β3 and β2, whereas γ1 was the main γ subunit (Fig. 1A). In single cell RNA-Seq (Fig. 1B), a similar result was obtained. Although α subunits did not present a clear preponderance, α3 was barely the major subunit, whereas β2, β3, and γ1 were well represented in the data sets. In both cases, γ2, γ3, β1, and δ, as well as α5 and α6 subunits, were expressed at low or below the limit of detection levels. These results, together with the analysis reported previously (Larson et al., 2016), are in agreement with previous functional studies (Arellano et al., 2016) suggesting that GABA$_A$Rs in OLs from neonate rats comprise a combination of α3/β2-β3/γ1-γ3 subunits. Based on this information, we amplified, cloned, and sequenced the five subunits from fresh OLs isolated from the rat optic nerve (P12) (Fig. 1C). The sequences obtained indicate that all subunits were identical to those expressed in other cell types including neurons. Thus, the α3 subunit in OL was identical to the sequence NP_058765.3 (Malherbe et al., 1990). The β2 and β3 sequences were identical to NP_037089.1 (Ymer et al., 1989) and NP_058761.1 (Ymer et al., 1989), respectively, whereas γ1 and γ3 corresponded to sequences NP_542153.1 (Ymer et al., 1990) and NP_077346.3 (Knoflach et al., 1991), respectively. Protein expression was confirmed by immunodetection in OPCs isolated from neonate forebrain for α3, α2, and γ1 subunits, but γ2 expression was not detected in the same preparations (Fig. 1D); as expected, the staining pattern for the analyzed subunits was different in cortical neuronal cells maintained in vitro (Supplemental Fig. 1).

The cRNA for each subunit was transcribed and injected into oocytes to express distinct receptor combinations as follows: $\alpha3\beta2$, $\alpha3\beta3$, $\alpha3\beta2\gamma1$, $\alpha3\beta2\gamma3$, $\alpha3\beta3\gamma1$, and $\alpha3\beta3\gamma3$. The functional characteristics of the receptors expressed were studied electrophysiologically to compare their behavior with that described for the endogenous $GABA_AR$ expressed in OL. First, D-R curves for GABA were built for each receptor within the concentration range of 100 nM to 1 mM (Fig. 2). All the subunit combinations expressed functional receptors, and the EC_{50} values estimated from the best fit for each normalized data set were as follows: $\alpha3\beta2$, 19 ± 4.18 μM; $\alpha3\beta3$, 10 ± 2.26 μM; $\alpha3\beta2\gamma1$, 53 ± 4 μM; $\alpha3\beta2\gamma3$, 21 ± 3.81 μM; $\alpha3\beta3\gamma1$, 58 ± 2.26 μM; and $\alpha3\beta3\gamma3$, 16 ± 2.22 μM (Fig. 2A). In all cases, the Hill coefficient (nH) was within the range of 0.82–1.33. Two main differences were observed: 1) the maximal current amplitude was obtained with the combination $\alpha3\beta2\gamma1$ that reached an average peak current of 9.37 ± 5.97 μA (n = 19 oocytes), whereas combinations $\alpha3\beta2\gamma3$ and $\alpha3\beta3\gamma1$ had peak currents of 2.36 ± 0.88 μA (n = 13 oocytes) and 4.43 ± 2.07 μA (n = 9 oocytes), respectively (Fig. 2B); and 2) the highest EC_{50} values were obtained for receptors containing the $\gamma1$ subunit. These values were statistically different ($P < 0.05$) from those observed in receptors without the γ subunit or with $\gamma3$ (Fig. 2C).

Sensitivity to Zn^{2+}. It has consistently been shown that GABA responses in OLs are inhibited by Zn^{2+} (100 μM; Williamson et al., 1998; Passlick et al., 2013; Arellano et al., 2016). This observation suggests the absence of the $\gamma2$ subunit, as it confers a relative insensitivity to the cation (Hosie et al., 2003; Trudell et al., 2008; Karim et al., 2013), whereas the absence of any γ subunit renders $GABA_ARs$ highly sensitive to Zn^{2+}. However, it is not known whether $\gamma1$ or $\gamma3$ confers insensitivity as well as $\gamma2$ does, especially in combination with the $\alpha3$ subunit. To achieve this information, we evaluated the effect of Zn^{2+} on the response elicited by GABA in oocytes expressing each of the combinations studied. Zn^{2+} and GABA were coapplied at 100 μM both, because this protocol inhibits more than 80% of the GABA response in receptors without γ subunits but has a weak effect on receptors with the $\gamma2$ subunit (e.g., Hosie et al., 2003; Karim et al., 2013). Figure 3 illustrates that the effect of Zn^{2+} on the peak of GABA response depended on the subunit combination expressed. Receptors without a γ subunit had the highest sensitivity to Zn^{2+} (67%–85% of inhibition), receptors with $\gamma3$ presented lower sensitivity (20%–32% of inhibition) and receptors with $\gamma1$ presented medium sensitivity to Zn^{2+} (within an inhibition range of 40%–50%). For comparison purposes, the current response of the receptor $\alpha3\beta2$ containing the $\gamma2$ subunit was inhibited around 10% in similar experiments. Thus, accordingly with several other studies where the participation of γ subunits greatly reduced the sensitivity to Zn^{2+}, this effect depended on the γ subunit type coexpressed in receptors containing $\alpha3\beta2$ or $\alpha3\beta3$ subunits. Among the different combinations tested in this condition, those that contained the $\gamma1$ subunit presented a medium sensitivity to Zn^{2+}. A more detailed analysis was made to assess the potency of Zn^{2+} on receptors expressing this subunit.

The sensitivity to Zn^{2+} of the endogenous receptor in OPCs and OLs is about 10 μM testing the GABA response around its

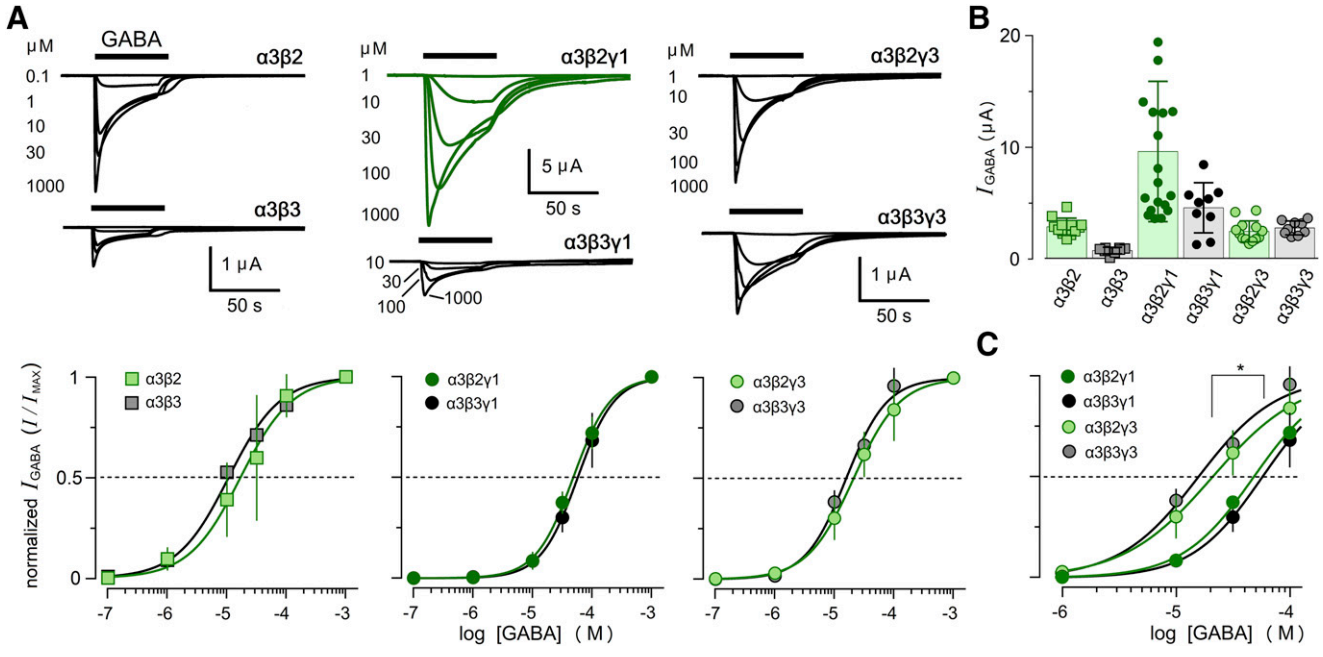

Fig. 2. Heterologous functional expression of oligodendroglial $GABA_AR$ subunits cloned from rat optic nerve. (A) The cRNA for $GABA_AR$ $\alpha3$, $\beta2$, $\beta3$, $\gamma1$, and $\gamma3$ subunits was synthesized and injected in different combinations into *Xenopus* oocytes as indicated. The expressed GABA responses were monitored electrophysiologically for each combination. In this and subsequent records, GABA was applied during the times indicated by bars at the top, and oocytes were held at −60 mV. D-R curves were constructed and plotted as illustrated; each point represents the average peak response (mean ± S.D.) normalized with respect to maximal current response elicited by 1 mM GABA monitored in 10–25 oocytes from three to five frogs. (B) Comparison of the peak current (mean ± S.D.) by 1 mM GABA generated in each of the combinations studied. Each bar includes 9–19 oocytes from five donors. $\alpha3\beta2\gamma1$ mean amplitude response was different to all others. (C) The graph built from data in (A) shows a comparison of the combinations containing $\alpha\beta\gamma$ subunits signaling the decrease in GABA sensitivity due to the presence of the $\gamma1$ subunit. The EC_{50} differences were statistically significant between the receptors containing $\gamma1$ vs. those containing $\gamma3$. *$P < 0.001$ for comparisons across the mean of $-\log EC_{50}$ values from each subunit combination, one-way ANOVA followed by a Tukey's post hoc test.

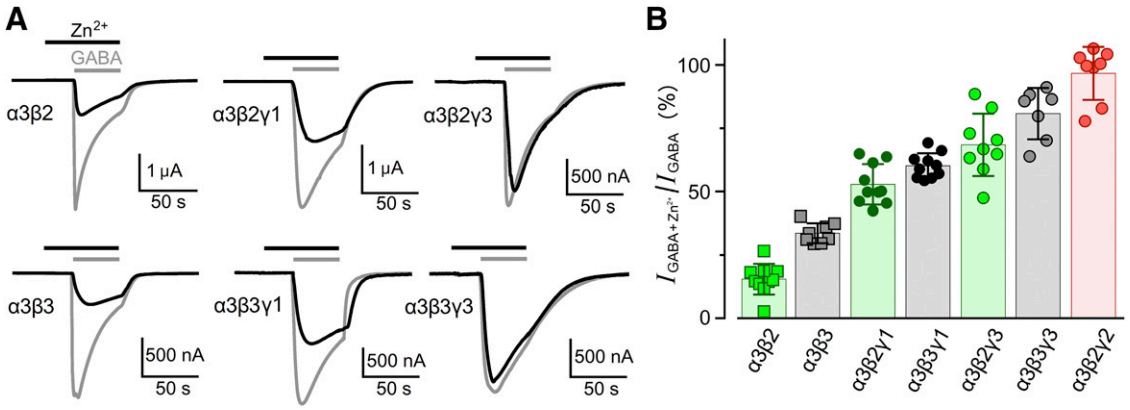

Fig. 3. Effect of Zn^{2+} on $GABA_A$Rs expressed in *Xenopus* oocytes from oligodendroglial sequences. (A) The traces illustrate the responses to 100 μM GABA in the absence (gray trace in each case) and presence of 100 μM Zn^{2+} (black trace) for each receptor studied as indicated. (B) The percentage of GABA response achieved in the presence of Zn^{2+} in each condition was normalized against the response generated without Zn^{2+}, then averaged and plotted in the bar graph (mean ± S.D.; 7–10 oocytes from three to five frogs). γ3 subunit conferred resistance to inhibition by Zn^{2+} similar to γ2 subunit, whereas presence of γ1 allowed inhibition of the GABA-response close to 50% and was statistically different to those receptors without γ subunit or containing either γ2 or γ3. One-way ANOVA ($P < 0.001$) followed by a post hoc Tukey test showed that all values were statistically different from each other.

EC_{10}–EC_{30} (Arellano et al., 2016). To compare the endogenous sensitivity with that displayed by heterologously expressed receptors, especially those containing the γ1 subunit, oocytes were injected with mRNA for $\alpha3\beta2\gamma1$ or $\alpha3\beta3\gamma1$ subunits, and these were compared with the receptor $\alpha3\beta2$. Responses for each combination were generated applying 10 μM GABA alone (control condition) or together with distinct Zn^{2+} concentrations within the range of 0.1–1000 μM (traces in Fig. 4A). Inhibition D-R curves were built for each receptor (Fig. 4B), normalizing the peak current response in the presence of Zn^{2+} against the maximal control response without Zn^{2+}. The half-maximal inhibitory concentration (IC_{50}) values obtained were of 6.2 ± 2.68, 25.7 ± 2.68, and 69 ± 3.13 μM (five to seven oocytes for each case) for the receptors $\alpha3\beta2$, $\alpha3\beta2\gamma1$, and $\alpha3\beta3\gamma1$, respectively; IC_{50} values were statistically different between all of them. This analysis shows that the receptor $\alpha3\beta2\gamma1$ had an IC_{50} similar to that displayed by the endogenous receptor (Arellano et al., 2016), whereas the $\alpha3\beta3\gamma1$ receptor was less sensitive, as well as the $\alpha3\beta2$ receptors in combination with either γ2 or γ3 subunit (Fig. 4C), which had an IC_{50} for Zn^{2+} of 82.7 ± 2.69 and 75.5 ± 2.91 μM, respectively.

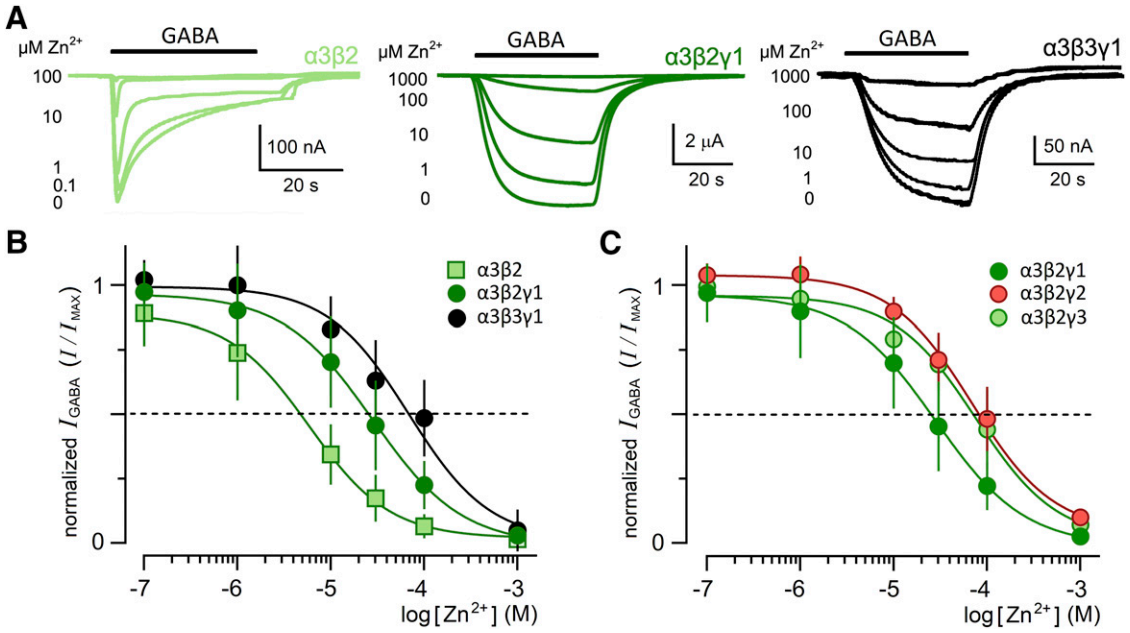

Fig. 4. D-R to Zn^{2+} of $GABA_A$Rs expressed in *Xenopus* oocytes from oligodendroglial sequences. (A) Top traces illustrate responses evoked by 10 μM GABA in the presence of different Zn^{2+} concentrations as indicated in each case for the $\alpha3\beta2$, $\alpha3\beta2\gamma1$, and $\alpha3\beta3\gamma1$ receptors expressed heterologously. (B, C) The response amplitude from recordings obtained in (A) were normalized with respect to the control GABA response, without Zn^{2+}, in the same oocytes, and the inhibition D-R curves were plotted to obtain the IC_{50} in each receptor. Data points represent the average (±S.D.) of five to seven oocytes (from three frogs) in each condition. Comparisons were made between the mean of the $-\log IC_{50}$ values of each combination of subunits. The one-way ANOVA ($P < 0.001$) followed by a post hoc Tukey test showed that all values were statistically different from each other.

Effect of Allosteric Modulators on the $\alpha3\beta2\gamma1$ $GABA_AR$. A battery of allosteric modulators was analyzed on the $\alpha3\beta2\gamma1$ receptor expressed in *Xenopus* oocytes, considering that this combination presented closer parameters of sensitivity to GABA and Zn^{2+} than those exhibited by receptors endogenously expressed in OLs; this combination is also in accordance with the transcriptomic analysis reported. The positive modulators DZP, indiplon, and β-CCB were analyzed by applying the respective EC_{10} for GABA, as a control response, and the same concentration of GABA in coapplication with each drug. Each modulator was applied alone for 40 seconds prior to coapplication with GABA (Fig. 5A). Both DZP and β-CCB enhanced the response to GABA by 198.0% ± 37.2% (11 oocytes) and 236.4% ± 40% (11 oocytes), respectively, whereas indiplon had a weak or null effect on the response (110.5% ± 3.65%, 10 oocytes) (Fig. 5B). In general, the effect of these modulators on the receptor $\alpha3\beta2\gamma1$ were like those displayed by the endogenous $GABA_AR$ expressed in OLs. The interaction of β-carboline with $\alpha3\beta2\gamma1$ was analyzed in greater detail (Fig. 5C). The positive effect of β-CCB (30 μM) was not blocked by FMZ (10 μM), a classic BZD site antagonist; in fact, application of FMZ together with β-CCB caused a greater response of the $\alpha3\beta2\gamma1$ receptor, as illustrated in Fig. 5C. Thus, the enhancement caused by β-CCB without FMZ was of 324.1% ± 74%, whereas in the presence of FMZ was of 446.9% ± 65% (17–20 oocytes in each case). This result suggested that the β-CCB binding site did not correspond to the classic BZD binding site, an observation that was supported by similar coapplication experiments with β-CCB and GABA at $\alpha3\beta2\gamma3$ and especially $\alpha3\beta2$ receptors in which the β-carboline also caused an important increase of the response (Fig. 5D).

To confirm this result, the specific binding sites of high and low affinity to BZD were mutated on the $\alpha3$, $\beta2$, and/or $\gamma1$ subunits. Thus, the $\alpha3\beta2\gamma1$ receptor sensitivity to DZP was eliminated or strongly decreased similarly to the manner previously shown for the neuronal receptor (Benson et al., 1998; Walters et al., 2000; Middendorp et al., 2015). The results of these experiments are illustrated in Fig. 6. First, the H126R mutation in the $\alpha3$ subunit eliminated the sensitivity to 1 μM DZP (Benson et al., 1998). However, positive modulation caused by β-CCB (1 μM) on the response to GABA (10 μM) was not affected, being 144.8% ± 18% in the oocytes expressing the native receptor and 202.4% ± 17.4% in the mutated receptor $\alpha3$(H126R)$\beta2\gamma1$ (five to six oocytes from two frogs; Fig. 6A). Also, mutations $\alpha3$(S294I)$\beta2$(N264I)$\gamma1$(S282I) were made to eliminate one of the low-affinity BZD sites located in the transmembrane region (Walters et al., 2000), and this receptor was expressed to explore its sensitivity to 60 μM DZP and 1 μM β-CCB. The results illustrated in Fig. 6B indicate that the potentiation of the GABA (10 μM) response produced by coapplication of 60 μM DZP was greatly reduced in the mutant receptor $\alpha3$(S294I)$\beta2$(N264I)$\gamma1$(S282I) compared with the $\alpha3\beta2\gamma1$ receptor response. The values were 281.1 ± 25% for the latter and 172.3% ± 10% for the mutant receptor, where persistent potentiation in this case was more likely due to DZP interaction on the high-affinity site. However, β-CCB application to the $\alpha3$(S294I)$\beta2$(N264I)$\gamma1$(S282I) receptor maintained a positive modulatory effect and enhanced the response by 251.6% ± 10.5% versus the control native receptor that presented an increase of 160.1% ± 8% (10 oocytes). These data support the idea that β-CCB did not act on the classic BZD site of the $GABA_A$ $\alpha3\beta2\gamma1$ receptor, but also did not act on the described transmembrane low-affinity site for BZD.

Effect of β-Carbolines on the Endogenous Response to GABA in OLs and Neurons. The effect of β-CCB acting on a different binding site to that of high-affinity for BZP on

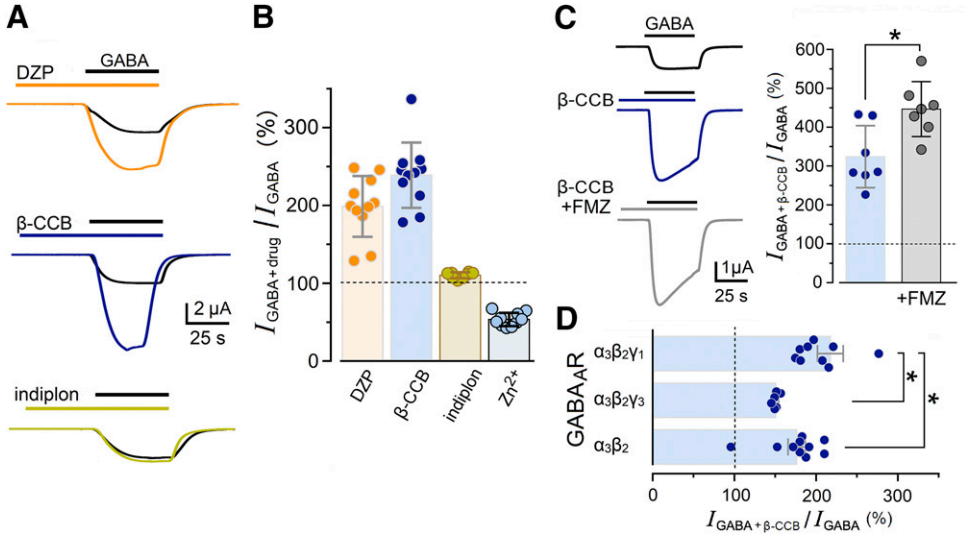

Fig. 5. Pharmacological effect of allosteric modulators on the GABA response of $\alpha3\beta2\gamma1$ receptors expressed in oocytes. (A) Traces illustrate the modulatory effect of drugs (10 μM; DZP, β-CCB, or indiplon) coapplied with GABA (10 μM) in each case; control response with GABA alone is shown in black. The mean effect response observed in 11 oocytes (five to six frogs) was plotted in (B) including the effect of Zn^{2+} in the same group of oocytes for comparison. (C) Traces illustrate the effect of 10 μM FMZ, a specific antagonist for the high affinity BZP binding site. It shows the response to 10 μM GABA alone, followed by the effect of 30 μM β-CCB in the absence and presence of FMZ that did not antagonize the enhancement caused by β-CCB. The mean effect response obtained in seven oocytes is shown in the bar graph. The increase in GABA response by β-CCB plus FMZ was statistically significant against the group without FMZ (*$P < 0.001$, paired two-tailed Student's t test). (D) Effect of 3 μM β-CCB on the GABA response activated in $\alpha3\beta2$ receptors without γ subunit, or those containing either $\gamma1$ or $\gamma3$. Mean responses (6–10 oocytes from three frogs) were statistically different for the three receptors compared with the control response elicited by GABA alone, and β-CCB enhancement in $\alpha3\beta2\gamma1$ response was different to all others. *$P < 0.001$ one-way ANOVA followed by a Tukey's post hoc test.

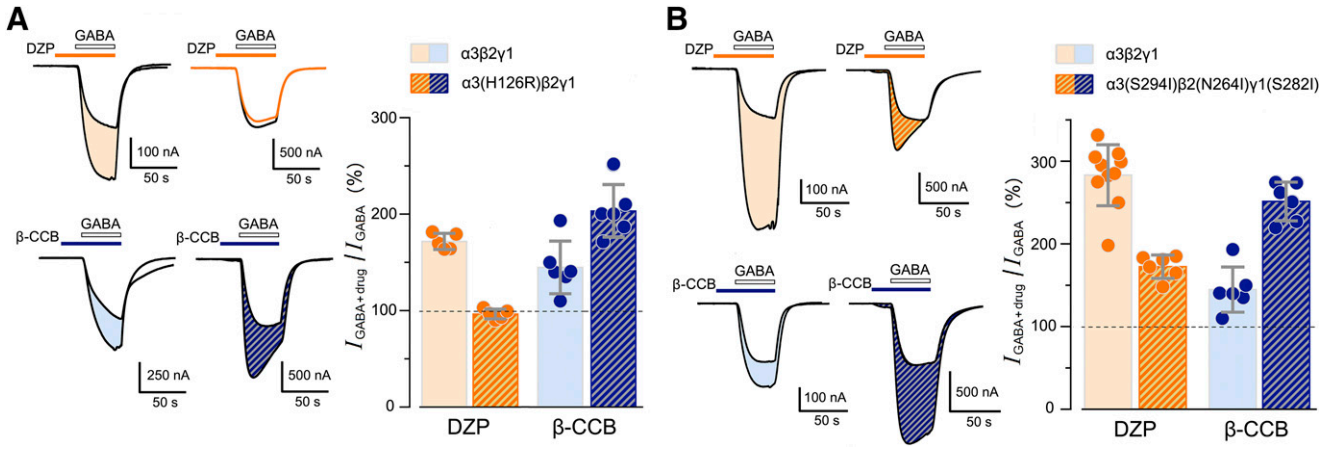

Fig. 6. The $\alpha3\beta2\gamma1$ receptor BZP binding sites and the enhancement caused by β-CCB. (A) 1 μM DZP or 3 μM β-CCB were coapplied with 10 μM GABA to analyze its effect on the high affinity site for BZP. Traces illustrate the responses obtained in oocytes that were injected with the cRNA of the native $\alpha3\beta2\gamma1$ subunits (left column), and in oocytes injected with the $\alpha3$(H126R)$\beta2\gamma1$ mutant (right column). The average responses obtained in five to six oocytes are shown in the bar graph indicating that DZP enhancement was eliminated, whereas the β-CCB enhancement was maintained in the mutated combination (line at 100% indicates control response to GABA). (B) Similar experiments in (A) were performed applying 60 μM DZP or 3 μM β-CCB coapplied with 10 μM GABA to analyze its effect on one of the low-affinity BZP sites. In the left column, the traces illustrate the responses obtained in oocytes expressing the native $\alpha3\beta2\gamma1$ subunits, whereas the second group expresses the mutant $\alpha3$(S294I)$\beta2$(N264I)$\gamma1$(S282I). The averages of the responses obtained in 10 oocytes (three frogs) are shown in the bar graph indicating that DZP enhancement was strongly reduced, whereas the increase generated by β-CCB was maintained in the mutated combination. All drug effects were statistically significant against the control group, with the clear exception of the mutant tested with DZP in (A) ($P < 0.001$ for comparisons between the control vs. drug-treated amplitude values, unpaired two-tailed Student's t test).

the $\alpha3\beta2\gamma1$ receptor is similar to the effect observed for the endogenous oligodendroglial GABA$_A$R. Figure 7 illustrates that the endogenous response to 10 μM GABA in cultured OLs isolated from optic nerve was enhanced by β-CCB (10 μM) but not affected by FMZ (10 μM) ($n = 7$). These results suggest that β-CCB did not act through the interaction with the high-affinity site for BZP in the endogenous GABA$_A$R in OLs. In contrast, FMZ did block the potentiation of the response to GABA mediated by DZP (10 μM) in either OLs ($n = 7$) or cortical neurons ($n = 5$) (Fig. 7A). Nevertheless, in this case FMZ did not cause an extra enhancement of the GABA response when tested in conjunction with β-CCB.

Also, it was observed that in the endogenous response, β-CCB enhancement was mainly due to an increase in the sensitivity to GABA, shown in Fig. 7B, where D-R curves for GABA were built in both the absence and presence of β-CCB (10 μM). Thus, in the absence of the modulator, the EC_{50} was of 83.3 $\pm$ 8.6 μM ($n = 5$), whereas in the presence of β-CCB, the EC_{50} was of 18.5 $\pm$ 3.4 μM ($n = 6$), the EC_{50} differences were statistically significant (*$P < 0.001$ for comparisons across the mean of $-\log EC_{50}$ values from each group; one-way ANOVA followed by a Tukey's post hoc test). The last EC_{50} value was also similar to that observed in the presence of β-CCB for the $\alpha3\beta2\gamma1$ receptor heterologously expressed.

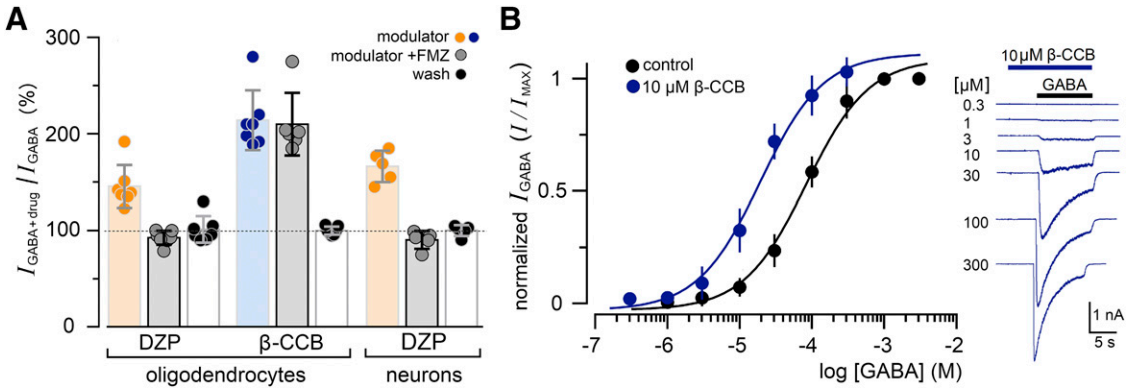

Fig. 7. β-CCB modulatory effect on the GABA response elicited in the oligodendroglial lineage. (A) GABA current response was monitored electrophysiologically in OLs (from optic nerve) or cortical neurons held at -80 mV. The enhancement mediated by either 10 μM DZP (orange bar) or 10 μM β-CCB (blue bar), in the presence and absence of 10 μM FMZ, was analyzed as summarized in the bar graph. The first black bar in each data set shows the control GABA response in the absence of drugs; the second bar of each group indicates the average of the response in the presence of a modulator; the gray bar indicates the modulator effect plus FMZ. The washing effect is in black. FMZ did not antagonize the response to β-CCB in OLs, but it was strongly effective on the potentiating DZP effect in both OLs and cortical neurons (10 μM GABA was used for OLs and 3 μM GABA for neurons). (B) D-R curves for GABA in OLs in the absence (black) and presence of 10 μM β-CCB (blue). Each data point represents the average response to GABA in eight OLs in both conditions. Data were adjusted to a D-R curve. Traces to the right illustrate the GABA current response in the presence of 10 μM β-CCB; in this and subsequent records in neural cells, drugs were applied as indicated by the top bars and cells were held at -80 mV.

A particularly important aspect of β-carboline action is the probable differential effect on the oligodendroglial receptor, compared with the effect on receptors expressed in neurons. To obtain more information about this effect, the potency for different β-carbolines on GABA responses in both OLs and cortical neurons maintained in culture was explored. It has been shown that β-CCB distinguishes between the receptors expressed in these two cell types (Cisneros-Mejorado et al., 2019). Here we confirmed this differential effect analyzing the effect of a battery of distinct β-carbolines on the endogenous GABA response of OLs and neurons. Figure 8 illustrates that the endogenous response to GABA in OLs or neurons (EC_{10} in each case) was monitored in the absence (control response) or presence of one of distinct β-carbolines. The normalized response with respect to the control is indicated as an average of the effect in the tested cells. The β-carboline (10 μM) positive modulatory effect on the response to GABA (10 μM) in OLs presented the following power sequence: β-CCB > β-carboline-3-carboxylic acid N-methylamide > β-CCE > tert-butyl β-carboline-3-carboxylate > β-CHM (Fig. 8A), whereas DMCM inhibited the response. In contrast, most of the β-carbolines (same concentration) presented either a net inhibitory effect on the neuronal receptor activated by 3 μM GABA or did not have a clear effect on the amplitude of the response, as observed for β-CCB or β-CCE (Fig. 8B). Thus, it appears that distinct β-carbolines presented a differential effect on the oligodendroglial $GABA_AR$. For β-CCB, this effect was not due to its interaction with the high-affinity binding site for BZP.

Specific Silencing of Endogenous α3 or γ1 $GABA_AR$ Subunits in OLs. Since α3 and γ1 subunits appear to define important characteristics of the endogenous oligodendroglial receptor, we performed the following experiments to directly determine their participation in the receptor conformation. For this, transfections with specific siRNA were performed for each subunit in OPCs isolated from neonate forebrain. Before performing the GABA response analysis in the transfected cells, OPCs were monitored for at least 4 days in vitro to evaluate essential characteristics such as marker expression (NG2, PDGFRα, MBP) and the electrophysiological and pharmacological GABA response profile. This was necessary because the maximal silencing effect of the respective protein had a 48-hour temporality. The result of this analysis indicated that most (85%–90%) cells maintained in culture from 2 DIV to 4 DIV in proliferating medium showed characteristics corresponding to OPCs expressing Olig2, NG2, and PDGFRα, but not glial fibrillary acidic protein or MBP, whereas at 4 DIV a significative percentage (21.6% ± 4.85%) of cells expressed O4 and presented a more complex morphology (Supplemental Fig. 2). Importantly, the $GABA_AR$ functional and pharmacological profile expressed did not change during the culture time from 2 DIV to 4 DIV. The current-voltage electrophysiological profile did not show statistically significant differences either (Supplemental Fig. 3), especially with regard to the typical rectifying behavior, due to the lack of Kir-type current activated at hyperpolarizing potentials (Pérez-Samartín et al., 2017). Thus, OPCs at 2 DIV were transfected with specific siRNA against either α3 (Fig. 9) or γ1 (Fig. 10) subunits, and the effect of this manipulation was compared with respect to cells that were transfected with a nonspecific siRNA (control), using the expression in untreated cells as reference. As illustrated in Fig. 9A, α3-siRNA transfection strongly reduced (93.7% ± 2%) the expression of the respective subunit as evidenced by the corresponding immunodetection, whereas transfection with nonspecific siRNA did not cause a notable α3 subunit expression decrease. The

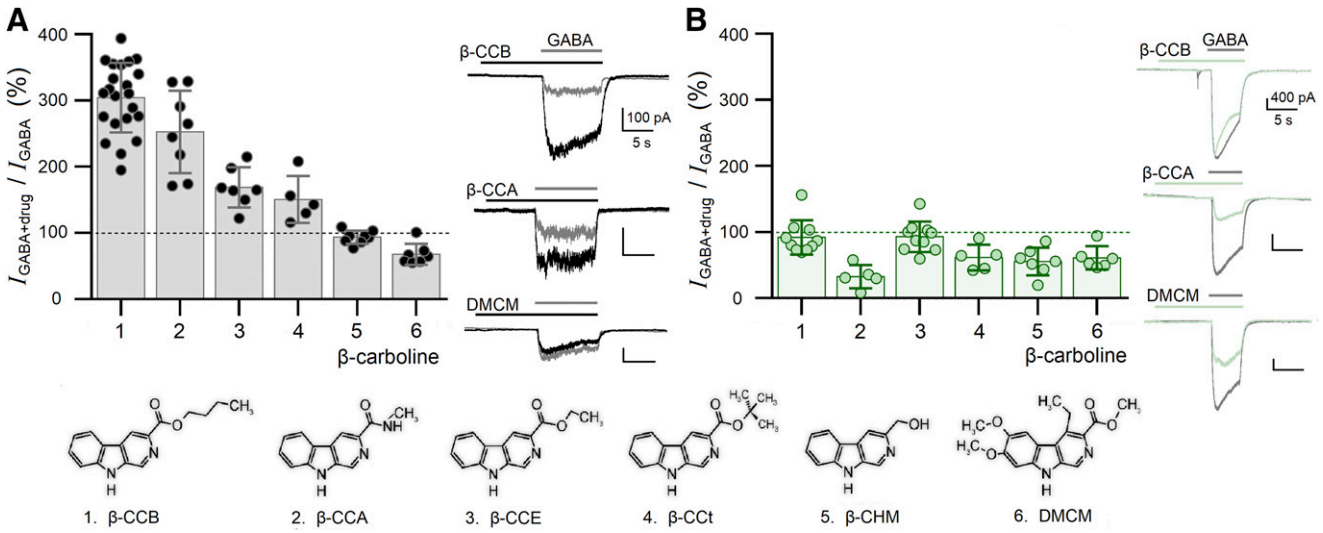

Fig. 8. β-carbolines modulatory effect on GABA current responses from either OLs or cortical neurons. (A) The response to 10 μM GABA in the absence and presence of a β-carboline (10 μM) was tested in OLs from the optic nerve. Each drug indicated from one to six corresponds to the structures in the lower part of the Figure, and traces illustrate the current response obtained for three drugs tested as indicated. Bars are the average of the normalized response with respect to the control response without β-carboline (100% line in graph) for each of the cells registered (6–21 cells in each case). The traces in gray correspond to control current responses, whereas black traces are the GABA responses in the presence of a β-carboline. (B) For comparison, a similar analysis was performed for the GABA response elicited in cortical neurons (six to eight cells in each case) by applying 3 μM GABA and the same set of β-carbolines. Traces illustrate responses obtained for the three drugs indicated, in gray correspond to control current responses, whereas green traces are the GABA responses in the presence of a β-carboline. All drug effects were statistically significant against the control group with exception of β-CHM in OLs, as well as β-CCB and β-CCE in neurons ($P < 0.001$ for comparisons between the control cells vs. β-carboline treated cells, unpaired two-tailed Student's t test). β-CCA, β-carboline-3-carboxylic acid N-methylamide; β-CCt, tert-butyl β-carboline-3-carboxylate.

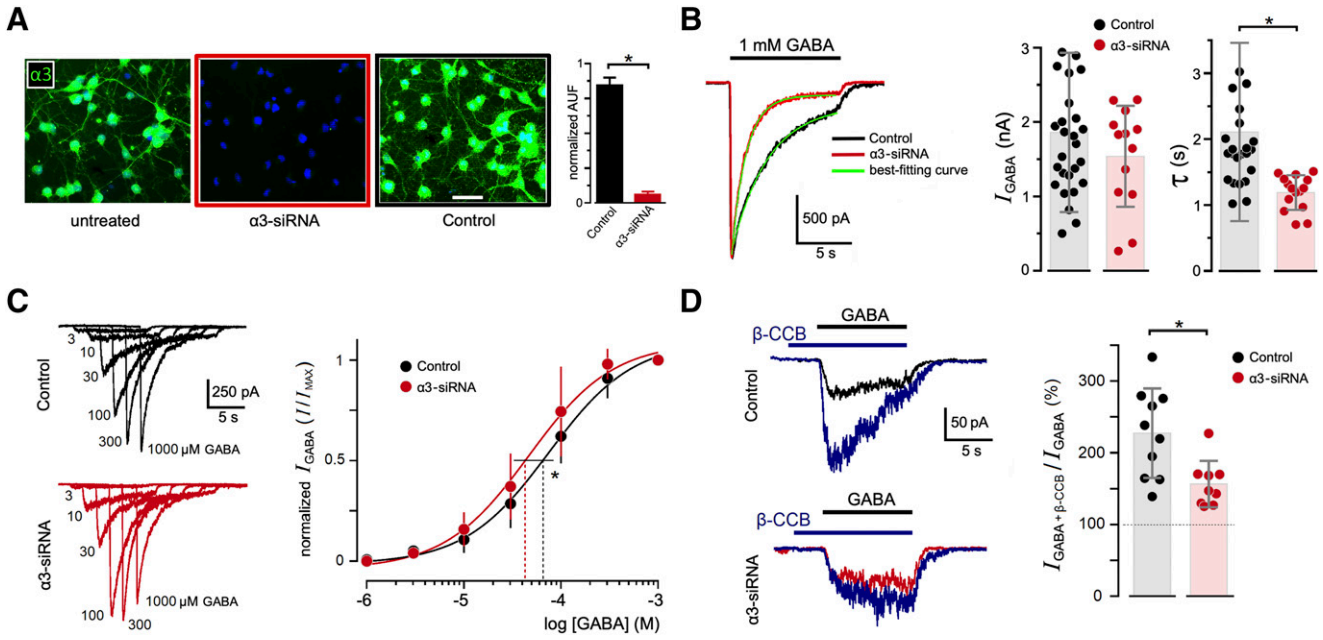

Fig. 9. α3 GABA$_A$R subunit silencing in cells of the oligodendroglial lineage. (A) Images illustrate α3 subunit immunodetection (in green, nuclei in blue) in OPCs maintained in culture. The first panel depicts cells without treatment (untreated). The cells designated as α3-siRNA were transfected with specific interfering sequences against the subunit, whereas control cells were processed for transfection with scramble sequences. All groups correspond to cells 72 hours after the transfection process. The estimated α3 expression in AUF was normalized with respect to the untreated group as shown in the bar graph (average of seven slices from three transfected cultures). (B) Analysis of responses evoked by 1 mM GABA in control and α3-siRNA treated cells. Traces correspond to typical records in both conditions where the desensitization kinetics was adjusted to an exponential curve to estimate the time constant (τ) decay, and the graphs show the amplitude response and τ values for each group, where each data point represents the response of one cell. The mean ± S.D. is shown in gray in each case. (C) Traces illustrate GABA D-R curves built for both groups; in the graph, each data point represents the mean ± S.D. of the normalized response in 10 cells. Lines are the best fit to D-R curves and broken lines indicate the corresponding EC_{50}. (D) Traces illustrate typical response in control (black), and α3-siRNA treated cells (red) evoked by GABA (10 μM) alone, or coapplied with 10 μM of β-CCB (blue trace). Bar graph shows the amplitude (mean ± S.D., in gray) response values for each group, where each data point represents the response in a single cell. *$P < 0.001$ for comparisons between the control cells vs. α3-siRNA treated cells, unpaired two-tailed Student's t test.

current amplitude generated by 1 mM GABA showed no change between these cell groups (1795.4 ± 1393 pA in control cells vs. 1539.3 ± 653 pA in α3-siRNA treated cells), although the GABA response showed three important changes. First, α3-siRNA treated cells showed an increase in the GABA response desensitization rate, as illustrated in Fig. 9B. This figure shows that control cells displayed a response desensitization fitted to an exponential decay with a mean time constant of 2109.2 ± 1321 millisecond, whereas the transfected cells presented desensitization time constants with an average of 1190 ± 253 millisecond (15–25 cells in each group; from four distinct transfections). Second, D-R curves constructed for these two experimental groups (Fig. 9C) showed that α3 subunit silencing caused an increase in the sensitivity of the expressed receptor and that the control EC_{50} of 75.1 ± 4.12 μM decreased to 46.6 ± 3.8 μM in α3-siRNA transfected cells (n = 10), a statistically significant difference. And third, α3-siRNA transfected cells also showed a decrease in sensitivity to β-CCB (10 μM) coapplied with GABA (10 μM) and generated a weaker increase of the GABA response to 156.4% ± 32.2% (nine cells) compared with the control effect of 227.26% ± 62.2% (10 cells), as illustrated in Fig. 9D.

γ1 subunit silencing in OPCs also caused changes, and although γ1 protein expression was not reduced by γ1-siRNA transfection as strongly as that designed against α3, the effect reached a 71 ± 1.6% decrease at 4 DIV as evidenced by immunodetection (Fig. 10, A and B). However, the γ1 expression decrease was accompanied by an average amplitude diminution of GABA (1 mM) peak response compared with the respective control of 55.1% ± 1.5% (1795.4 ± 1393 vs. 805.6 ± 463 pA). In this case, the corresponding EC_{50} values for both groups did not show a statistically significant difference (75.1 ± 4.12 μM for the control group vs. 88.9 ± 3.48 μM for γ1-siRNA transfected cells; 10–15 cells in each case, four different transfections) (Fig. 10C). In similar manner to that showed for α3-siRNA transfected cells, the γ1-siRNA transfected cells were less sensitive to β-CCB, and in the presence of the β-carboline the GABA-response was barely enhanced to 113.2% ± 16.6%, whereas the control group (same than control in Fig. 9D) was increased to 227% (Fig. 10D). These results showed that both subunits, α3 and γ1, seem to participate in the conformation of the endogenous receptor. They also suggested that the absence of α3 was compensated by another subunit, whereas γ1 subunit expression was essential to maintain the GABA response in OPCs as well as their sensitivity to β-CCB.

Discussion

The molecular mechanisms responsible for the control of myelination are only partially known, and their definition will help to identify new therapeutic targets for the treatment of various pathologic conditions. GABA signaling participates in myelination (Zonouzi et al., 2015; Arellano et al., 2016; Balia et al., 2017; Hamilton et al., 2017; Kalanjati et al., 2017; Shaw et al., 2018; Cisneros-Mejorado et al., 2019; Kalakh and

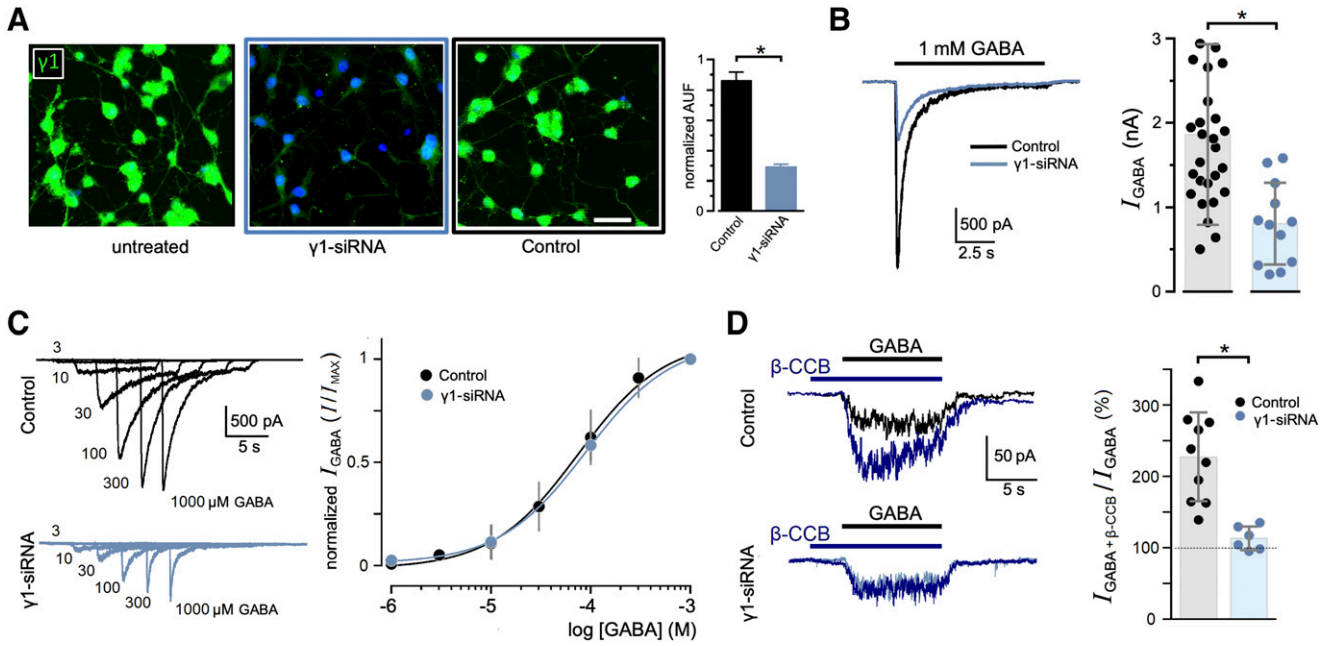

Fig. 10. γ1 $GABA_AR$ subunit silencing in cells of the oligodendroglial lineage. (A) Images illustrate γ1 subunit immunodetection (in green, nuclei in blue) in OPCs maintained in culture. The first panel shows the untreated cells. The γ1-siRNA group represents cells transfected with specific interfering sequences against the subunit. Control cells were processed for transfection with scramble sequences. (B) After 72 hours, the expression of γ1 was estimated in AUF, and the values were normalized with respect to the untreated group (average of seven slices from three transfected cultures). Also, traces illustrate responses elicited by 1 mM GABA in control and γ1-siRNA treated cells. The response amplitude for each group is represented in the graph. Each data point is the amplitude obtained in a single cell, and the mean ± S.D. is indicated in gray. (C) Traces illustrate GABA D-R curves built for both groups, where each data point represents the mean ± S.D. of the normalized response in 17–20 cells, and lines are the best fit to D-R curves. (D) Traces illustrate typical response in control (black), and γ1-siRNA treated cells (light blue) evoked by GABA (10 μM) alone, or coapplied with 10 μM of β-CCB (dark blue trace). Bar graph shows the amplitude (mean ± S.D., in gray) response values for each group, where each data point represents the response in a single cell. *$P < 0.001$ for comparisons between the control cells vs. γ1-siRNA treated cells, unpaired two-tailed Student's t test.

Mouihate, 2019; Serrano-Regal et al., 2019); however, its specific functional role and mechanisms involved are not completely understood. To progress in these issues, this study aimed to determine the molecular identity of the main $GABA_AR$ expressed in the oligodendroglial lineage, especially in OPCs and OLs from newborn rats (Arellano et al., 2016). The results indicated that the receptor composition includes the α3 and γ1 subunits, whereas the most likely β subunit involved is β2. The identity proposed here, α3β2γ1, agrees with other studies proposing a composition α3/β2 or β3/γ1 or γ3 from a pharmacological and functional perspective (Arellano et al., 2016), and with the transcriptomic analysis performed in $NG2^+$ cells (Larson et al., 2016), where the mentioned subunits have a high expression level. The transcriptomic analysis presented here in PDGFRα$^+$ cells confirmed the expression of the coding sequences for various subunits, where the α2 and α3 subunits, together with β2, β3, and γ1, were all well represented. This analysis also highlighted the low or null expression of γ2, γ3, and δ subunits. Thus, coincidentally, a similar group of subunits was suggested from all the transcriptomic analyzes described and the set of subunits proposed from the functional studies, regardless of the murine species, age, and brain region. This concordance supports the relevant contribution of α3, β2, and γ1 subunits to $GABA_AR$ in cultured OLs from the neonatal brain but clearly does not exclude participation of other subunits for which solid evidence of their expression has been found in certain areas of the nervous system and in different stages of development (Passlick et al., 2013; see also Serrano-Regal et al., 2020).

$GABA_AR$ subunits protein expression was confirmed by immunodetection in cultured OLs and OPCs from the forebrain, and transcripts of α3, β2, β3, γ1, and γ3 subunits were subsequently amplified from OLs isolated and purified from rat optic nerve; the corresponding genes were cloned, and cRNA synthesized in vitro was expressed into *X. laevis* oocytes to analyze the functional characteristics of six possible receptors. Their characteristics were compared with those shown by the endogenous receptors reported previously (e.g., Arellano et al., 2016) to determine which combination most closely reproduced the endogenous GABA response. Results studying GABA sensitivity showed that α3β2γ1 was the most efficient in terms of amplitude response; it remains unknown if this represents an intrinsic condition for preferential assemble. However, it is important to note that substitution of β2 by β3 results in an important decrease in the amplitude of the GABA responses.

$GABA_ARs$ with α3β2γ1 subunits have an EC_{50} of 53 μM. Substitution of β2 by β3 in this combination did not change GABA responses, whereas substitution of γ1 by γ3 caused a threefold increase in GABA sensitivity. Hence, the EC_{50} value for the heterologously expressed α3β2γ1 is close to that of the endogenous receptor, as all reports so far indicate an EC_{50} for GABA between 70 and 100 μM (e.g., Arellano et al., 2016).

On the other hand, Zn^{2+} sensitivity is a key parameter for this comparison because high sensitivity is an indicator of γ subunit absence. It was demonstrated that compared with γ2 and γ3 subunits, γ1 confers moderate Zn^{2+} sensitivity; furthermore, it was also clear that β subunit substitution also

affected this parameter. The receptors containing the $\gamma1$ subunit were studied further, applying (10 μM) GABA and constructing D-R curves for Zn^{2+}. The $\alpha3\beta2\gamma1$ conformation presented an IC_{50} of 25 μM, which was similar to the value observed in the endogenous receptor, whereas the substitution of $\beta2$ by $\beta3$ increased threefold this parameter. Therefore, the combination containing $\beta2$ is closer to the endogenous value. Additionally, by comparing the IC_{50} values for receptors containing the combination $\alpha3\beta2$ with, or without a γ subunit, once again $\alpha3\beta2\gamma1$ presented the closest IC_{50} value to that described for the endogenous receptor.

The combination $\alpha3\beta2\gamma1$ also presented an endogenous-like sensitivity for allosteric modulators, such as DZP, indiplon, and the β-carboline β-CCB. The β-CCB effect is important because it distinguishes between receptors expressed either in OLs or neurons. Given that this drug has the potential for specifically promoting GABAergic signaling in OLs in vivo (Arellano et al., 2016; Cisneros-Mejorado et al., 2019), it was critical to explore in detail the action of β-CCB on the $\alpha3\beta2\gamma1$ receptor. Results indicated that β-CCB effect did not require interaction with the classic BZP binding site, since it was not antagonized by FMZ. Instead, FMZ caused a greater enhancement, suggesting, as proposed before (Sieghart, 2015), that β-CCB had a dual effect in which the classic site promoted inhibition (i.e., the inverse agonist effect) and a second site caused the positive modulatory effect. Studies have suggested that this potentiation site for β-carbolines might include residues conforming the low-affinity binding site for DZP located in the second transmembrane domains of α, β, and γ subunits (Walters et al., 2000). This is supported by results showing that the $\alpha3\beta2$ receptor is still potentiated by β-CCB. Because subunit substitution might represent a more complex change in the final binding site configuration, we performed point mutations in $\alpha3\beta2\gamma1$ to eliminate the high and low affinity DZP binding sites. Mutations eliminated DZP sensitivity as described for $\gamma2$-containing receptors (Benson et al., 1998; Walters et al., 2000); however, β-CCB was still effective as an enhancer in both mutants, indicating that its effect was not due to interaction with the proposed sites; thus, the β-CCB binding site acting as enhancer on $\alpha3\beta2\gamma1$ remains unknown. The $GABA_AR$ in OLs presented similar behavior with respect to the DZP high-affinity binding site, since the β-CCB positive modulatory effect was not antagonized by FMZ. This adds evidence supporting the idea that $\alpha3\beta2\gamma1$ and the endogenous receptor are similar.

The modulatory effect on the endogenous receptor by β-CCB was due to a fivefold increase in GABA sensitivity. Distinct β-carbolines presented differential potency on the oligodendroglial receptor, drugs that generated a net potentiating effect on the GABA response in OLs, such as β-CCB or β-CCE, did not have a prominent effect in neurons; thus, they can potentially be used as drugs to differentially stimulate GABAergic signaling in OLs. Lipophilicity of the β-carboline seems to be determinant for the interaction with the receptor, a highly lipophilic drug such as β-CCB had the greatest positive effect, whereas the most hydrophilic DMCM turns to be inhibitory in both cell types. This suggests that the enhancer binding site has relation with the receptor lipophilic microenvironment; thus probably the specific composition of the oligodendroglial and neuronal membranes would influence on the degree of inhibition or enhancement observed for the different drugs, a distinct lipidic microenvironment might also explain some differences observed using the heterologous expression model.

To give greater certainty about the participation of both $\alpha3$ and $\gamma1$ subunits, these were specifically silenced in OPCs. Subunit silencing strongly decreased the corresponding protein expression and substantially changed the OPC GABA response. $\alpha3$ subunit silencing altered GABA sensitivity of the expressed receptor, as well as the receptor desensitization kinetics and the sensitivity to β-CCB. However, its peak amplitude remained unchanged, suggesting that the $\alpha3$ absence was compensated by some other subunit conforming a different receptor; $\alpha1$ and $\alpha2$ subunits are candidates for this because both are expressed in OPCs, which would explain the increase in GABA sensitivity and the desensitization rate. In contrast, $\gamma1$ silencing caused a clear decrease in amplitude response, suggesting that $\gamma1$ is essential for the $GABA_AR$ expression in the OPC membrane; thus, this subunit is a plausible target to be downregulated in experiments designed for the study of GABAergic signaling function during the myelination process.

Together, these results provide pharmacological (use of β-carbolines) and genetic information that can be used to generate changes in the effectiveness of the $GABA_AR$ expressed in OLs and their precursor cells in the neonatal stage, which could be crucial to modify the status of GABAergic signaling in the context of its interaction with neurons during the first peak of myelination. The transcriptomic analyzes suggest that the proposed subunits remain well represented in OPCs until the adulthood; it is therefore likely that these subunits will be involved throughout life. Given that other subunits are coexpressed and that clearly there are differences of expression in different areas, participation of some other subunits cannot yet be completely ruled out.

Thus, evidence indicates that the endogenous $GABA_AR$ expressed in oligodendroglial lineage cells, from its OPC stage to premyelinating OLs, most likely contains the $\alpha3$, $\beta2$, and $\gamma1$ subunits; this contributes to the determination of the oligodendroglial receptor structure that will allow molecular studies to characterize its function in the myelination process.

Acknowledgments

We thank Jessica González Norris for editing this manuscript. We also thank Felipe Cornejo Ortiz, Dra. Nuri Aranda López, Lic. Ma. de Lourdes Lara Ayala, Ing. Elsa Nydia Hernández Ríos, M.V.Z. Martín García Servín, Alejandra Castilla León, Francisco J. Valles Valenzuela, and Ing. Ramón Martínez Olvera for their expert technical support. A.C.-M. is a researcher from Cátedras-CONACYT commissioned at Instituto de Neurobiología in the Universidad Nacional Autónoma de México (UNAM). R.P.O. is a doctoral student from Programa de Doctorado en Ciencias Biomédicas of the Universidad Nacional Autónoma de México (UNAM) and received fellowship no. 700811 from CONACYT, México.

Authorship Contributions

Participated in research design: Ordaz, Garay, Limon, Matute, Arellano.

Conducted experiments: Ordaz, Garay, Pérez-Samartín, Sánchez-Gómez, Robles-Martínez, Cisneros-Mejorado, Matute, Arellano.

Performed data analysis: Ordaz, Garay, Limon, Pérez-Samartín, Sánchez-Gómez, Cisneros-Mejorado, Matute, Arellano.

Wrote or contributed to the writing of the manuscript: Ordaz, Garay, Limon, Pérez-Samartín, Sánchez-Gómez, Robles-Martínez, Cisneros-Mejorado, Matute, Arellano.

References

Arellano RO and Miledi R (1993) Novel Cl^- currents elicited by follicle stimulating hormone and acetylcholine in follicle-enclosed *Xenopus* oocytes. *J Gen Physiol* **102**: 833–857.

Arellano RO, Sánchez-Gómez MV, Alberdi E, Canedo-Antelo M, Chara JC, Palomino A, Pérez-Samartín A, and Matute C (2016) Axon-to-glia interaction regulates $GABA_A$ receptor expression in oligodendrocytes. *Mol Pharmacol* **89**:63–74.

Attali B, Wang N, Kolot A, Sobko A, Cherepanov V, and Soliven B (1997) Characterization of delayed rectifier Kv channels in oligodendrocytes and progenitor cells. *J Neurosci* **17**:8234–8245.

Balia M, Benamer N, and Angulo MC (2017) A specific GABAergic synapse onto oligodendrocyte precursors does not regulate cortical oligodendrogenesis. *Glia* **65**: 1821–1832.

Balia M, Vélez-Fort M, Passlick S, Schäfer C, Audinat E, Steinhäuser C, Seifert G, and Angulo MC (2015) Postnatal down-regulation of the $GABA_A$ receptor $\gamma 2$ subunit in neocortical NG2 cells accompanies synaptic-to-extrasynaptic switch in the GABAergic transmission mode. *Cereb Cortex* **25**:1114–1123.

Baraban M, Koudelka S, and Lyons DA (2018) Ca^{2+} activity signatures of myelin sheath formation and growth in vivo. *Nat Neurosci* **21**:19–23.

Benson JA, Löw K, Keist R, Mohler H, and Rudolph U (1998) Pharmacology of recombinant γ-aminobutyric acidA receptors rendered diazepam-insensitive by point-mutated α-subunits. *FEBS Lett* **431**:400–404.

Bronstein JM, Hales TG, Tyndale RF, and Charles AC (1998) A conditionally immortalized glial cell line that expresses mature myelin proteins and functional $GABA_{(A)}$ receptors. *J Neurochem* **70**:483–491.

Cahoy JD, Emery B, Kaushal A, Foo LC, Zamanian JL, Christopherson KS, Xing Y, Lubischer JL, Krieg PA, Krupenko SA, et al. (2008) A transcriptome database for astrocytes, neurons, and oligodendrocytes: a new resource for understanding brain development and function. *J Neurosci* **28**:264–278.

Cesetti T, Ciccolini F, and Li Y (2012) GABA not only a neurotransmitter: osmotic regulation by GABA(A)R signaling. *Front Cell Neurosci* **6**:3.

Cheli VT, Santiago González DA, Namgyal Lama T, Spreuer V, Handley V, Murphy GG, and Paez PM (2016) Conditional deletion of the L-type calcium channel $Ca_V1.2$ in oligodendrocyte progenitor cells affects postnatal myelination in mice. *J Neurosci* **36**:10853–10869.

Cheli VT, Santiago González DA, Spreuer V, and Paez PM (2015) Voltage-gated Ca^{2+} entry promotes oligodendrocyte progenitor cell maturation and myelination *in vitro*. *Exp Neurol* **265**:69–83.

Cisneros-Mejorado AJ, Garay E, Ortiz-Retana J, Concha L, Moctezuma JP, Romero S, and Arellano RO (2019) Demyelination–remyelination of the rat caudal cerebellar peduncle evaluated with magnetic resonance imaging. *Neuroscience* **439**: 255–267.

Dumont JN (1972) Oogenesis in *Xenopus laevis* (Daudin). I. Stages of oocyte development in laboratory maintained animals. *J Morphol* **136**:153–179.

Gilbert P, Kettenmann H, and Schachner M (1984) gamma-Aminobutyric acid directly depolarizes cultured oligodendrocytes. *J Neurosci* **4**:561–569.

Hamilton NB, Clarke LE, Arancibia-Carcamo IL, Kougioumtzidou E, Matthey M, Káradóttir R, Whiteley L, Bergersen LH, Richardson WD, and Attwell D (2017) Endogenous GABA controls oligodendrocyte lineage cell number, myelination, and CNS internode length. *Glia* **65**:309–321.

Hoppe D and Kettenmann H (1989) GABA triggers a Cl^- efflux from cultured mouse oligodendrocytes. *Neurosci Lett* **97**:334–339.

Hosie AM, Dunne EL, Harvey RJ, and Smart TG (2003) Zinc-mediated inhibition of $GABA_{(A)}$ receptors: discrete binding sites underlie subtype specificity. *Nat Neurosci* **6**:362–369.

Jabs R, Pivneva T, Hüttmann K, Wyczynski A, Nolte C, Kettenmann H, and Steinhäuser C (2005) Synaptic transmission onto hippocampal glial cells with hGFAP promoter activity. *J Cell Sci* **118**:3791–3803.

Kalakh S and Mouihate A (2019) Enhanced remyelination during late pregnancy: involvement of the GABAergic system. *Sci Rep* **9**:7728.

Kalanjati VP, Wixey JA, Miller SM, Colditz PB, and Bjorkman ST (2017) $GABA_A$ receptor expression and white matter disruption in intrauterine growth restricted piglets. *Int J Dev Neurosci* **59**:1–9.

Káradóttir R, Hamilton NB, Bakiri Y, and Attwell D (2008) Spiking and nonspiking classes of oligodendrocyte precursor glia in CNS white matter. *Nat Neurosci* **11**: 450–456.

Karim N, Wellendorph P, Absalom N, Johnston GAR, Hanrahan JR, and Chebib M (2013) Potency of GABA at human recombinant $GABA_{(A)}$ receptors expressed in *Xenopus* oocytes: a mini review. *Amino Acids* **44**:1139–1149.

Kirchhoff F and Kettenmann H (1992) GABA triggers a $[Ca^{2+}]_i$ increase in murine precursor cells of the oligodendrocyte lineage. *Eur J Neurosci* **4**:1049–1058.

Knoflach F, Rhyner T, Villa M, Kellenberger S, Drescher U, Malherbe P, Sigel E, and Möhler H (1991) The γ 3-subunit of the $GABA_A$-receptor confers sensitivity to benzodiazepine receptor ligands. *FEBS Lett* **293**:191–194.

Krasnow AM, Ford MC, Valdivia LE, Wilson SW, and Attwell D (2018) Regulation of developing myelin sheath elongation by oligodendrocyte calcium transients *in vivo*. *Nat Neurosci* **21**:24–28.

Kukley M, Kiladze M, Tognatta R, Hans M, Swandulla D, Schramm J, and Dietrich D (2008) Glial cells are born with synapses. *FASEB J* **22**:2957–2969.

Larm JA, Cheung NS, and Beart PM (1996) (S)-5-fluorowillardiine-mediated neurotoxicity in cultured murine cortical neurones occurs via AMPA and kainate receptors. *Eur J Pharmacol* **314**:249–254.

Larson VA, Zhang Y, and Bergles DE (2016) Electrophysiological properties of $NG2^{(+)}$ cells: matching physiological studies with gene expression profiles. *Brain Res* **1638**:138–160.

Lin SC and Bergles DE (2004) Synaptic signaling between GABAergic interneurons and oligodendrocyte precursor cells in the hippocampus. *Nat Neurosci* **7**:24–32.

Malherbe P, Sigel E, Baur R, Persohn E, Richards JG, and Möhler H (1990) Functional expression and sites of gene transcription of a novel α subunit of the $GABA_A$ receptor in rat brain. *FEBS Lett* **260**:261–265.

Marques S, Zeisel A, Codeluppi S, van Bruggen D, Mendanha Falcão A, Xiao L, Li H, Häring M, Hochgerner H, Romanov RA, et al. (2016) Oligodendrocyte heterogeneity in the mouse juvenile and adult central nervous system. *Science* **352**: 1326–1329.

Middendorp SJ, Maldifassi MC, Baur R, and Sigel E (2015) Positive modulation of synaptic and extrasynaptic $GABA_A$ receptors by an antagonist of the high affinity benzodiazepine binding site. *Neuropharmacology* **95**:459–467.

Orduz D, Maldonado PP, Balia M, Vélez-Fort M, de Sars V, Yanagawa Y, Emiliani V, and Angulo MC (2015) Interneurons and oligodendrocyte progenitors form a structured synaptic network in the developing neocortex. *eLife* **4**:1–20.

Passlick S, Grauer M, Schäfer C, Jabs R, Seifert G, and Steinhäuser C (2013) Expression of the γ2-subunit distinguishes synaptic and extrasynaptic GABA(A) receptors in NG2 cells of the hippocampus. *J Neurosci* **33**:12030–12040.

Pérez-Samartín A, Garay E, Moctezuma JPH, Cisneros-Mejorado A, Sánchez-Gómez MV, Martel-Gallegos G, Robles-Martínez L, Canedo-Antelo M, Matute C, and Arellano RO (2017) Inwardly rectifying K^+ currents in cultured oligodendrocytes from rat optic nerve are insensitive to pH. *Neurochem Res* **42**:2443–2455.

Pitman KA and Young KM (2016) Activity-dependent calcium signalling in oligodendrocyte generation. *Int J Biochem Cell Biol* **77**:30–34.

Sánchez-Gómez MV, Serrano MP, Alberdi E, Pérez-Cerdá F, and Matute C (2018) Isolation, expansion, and maturation of oligodendrocyte lineage cells obtained from rat neonatal brain and optic nerve. *Methods Mol Biol* **1791**:95–113.

Sequeira A, Shen K, Gottlieb A, and Limon A (2019) Human brain transcriptome analysis finds region- and subject-specific expression signatures of $GABA_AR$ subunits. *Commun Biol* **2**:153.

Serrano-Regal MP, Luengas-Escuza I, Bayón-Cordero L, Ibarra-Aizpurua N, Alberdi E, Pérez-Samartín A, Matute C, and Sánchez-Gómez MV (2019) Oligodendrocyte differentiation and myelination is potentiated via $GABA_B$ receptor activation. *Neuroscience* **439**:163–180.

Serrano-Regal MP, Bayón-Cordero L, Ordaz RP, Garay E, Limon A, Arellano RO, Matute C, and Sánchez-Gómez MV (2020) Expression and function of GABA receptors in myelinating cells. *Front Cell Neurosci* **14**:256.

Shaw JC, Berry MJ, Dyson RM, Crombie GK, Hirst JJ, and Palliser HK (2019) Reduced neurosteroid exposure following preterm birth and its' contribution to neurological impairment: a novel avenue for preventative therapies. *Front Physiol* **10**:599.

Shaw JC, Palliser HK, Dyson RM, Berry MJ, and Hirst JJ (2018) Disruptions to the cerebellar GABAergic system in juvenile guinea pigs following preterm birth. *Int J Dev Neurosci* **65**:1–10.

Sieghart W (2015) Allosteric modulation of $GABA_A$ receptors via multiple drug-binding sites, in *Advances in Pharmacology* (Rudolph U, ed) pp 53–96, Elsevier Inc., Amsterdam.

Tanaka Y, Tozuka Y, Takata T, Shimazu N, Matsumura N, Ohta A, and Hisatsune T (2009) Excitatory GABAergic activation of cortical dividing glial cells. *Cereb Cortex* **19**:2181–2195.

Tasic B, Menon V, Nguyen TN, Kim TK, Jarsky T, Yao Z, Levi B, Gray LT, Sorensen SA, Dolbeare T, et al. (2016) Adult mouse cortical cell taxonomy revealed by single cell transcriptomics. *Nat Neurosci* **19**:335–346.

Trudell JR, Yue ME, Bertaccini EJ, Jenkins A, and Harrison NL (2008) Molecular modeling and mutagenesis reveals a tetradentate binding site for Zn2+ in GABA(A) alphabeta receptors and provides a structural basis for the modulating effect of the γ subunit. *J Chem Inf Model* **48**:344–349.

Vélez-Fort M, Audinat E, and Angulo MC (2012) Central role of GABA in neuron-glia interactions. *Neuroscientist* **18**:237–250.

Vélez-Fort M, Maldonado PP, Butt AM, Audinat E, and Angulo MC (2010) Postnatal switch from synaptic to extrasynaptic transmission between interneurons and NG2 cells. *J Neurosci* **30**:6921–6929.

Von Blankenfeld G, Trotter J, and Kettenmann H (1991) Expression and developmental regulation of a $GABA_A$ receptor in cultured murine cells of the oligodendrocyte lineage. *Eur J Neurosci* **3**:310–316.

Wake H, Ortiz FC, Woo DH, Lee PR, Angulo MC, and Fields RD (2015) Nonsynaptic junctions on myelinating glia promote preferential myelination of electrically active axons. *Nat Commun* **6**:7844.

Walters RJ, Hadley SH, Morris KD, and Amin J (2000) Benzodiazepines act on $GABA_A$ receptors via two distinct and separable mechanisms. *Nat Neurosci* **3**: 1274–1281.

Williamson AV, Mellor JR, Grant AL, and Randall AD (1998) Properties of $GABA_{(A)}$ receptors in cultured rat oligodendrocyte progenitor cells. *Neuropharmacology* **37**: 859–873.

Ymer S, Draguhn A, Wisden W, Werner P, Keinänen K, Schofield PR, Sprengel R, Pritchett DB, and Seeburg PH (1990) Structural and functional characterization of the γ 1 subunit of $GABA_A$/benzodiazepine receptors. *EMBO J* **9**:3261–3267.

Ymer S, Schofield PR, Draguhn A, Werner P, Köhler M, and Seeburg PH (1989) GABAA receptor beta subunit heterogeneity: functional expression of cloned cDNAs. *EMBO J* **8**:1665–1670.

Zhang Y, Chen K, Sloan SA, Bennett ML, Scholze AR, O'Keeffe S, Phatnani HP, Guarnieri P, Caneda C, Ruderisch N, et al. (2014) An RNA-sequencing transcriptome and splicing database of glia, neurons, and vascular cells of the cerebral cortex. *J Neurosci* **34**:11929–11947.

Zonouzi M, Scafidi J, Li P, McEllin B, Edwards J, Dupree JL, Harvey L, Sun D, Hübner CA, Cull-Candy SG, et al. (2015) GABAergic regulation of cerebellar NG2 cell development is altered in perinatal white matter injury. *Nat Neurosci* **18**:674–682.

Address correspondence to: Dr. Rogelio O. Arellano, Instituto de Neurobiología, Universidad Nacional Autónoma de México., Blvd. Juriquilla 3001, Juriquilla Querétaro, C.P. 76230, México. E-mail: arellano.ostoa@comunidad.unam.mx; or Dr. Carlos Matute, Dpto. Neurociencias, Universidad del País Vasco, E-48940 Leioa, Spain. E-mail: carlos.matute@ehu.eus

$GABA_A$ RECEPTORS EXPRESSED IN OLIGODENDROCYTES CULTURED FROM THE NEONATAL RAT CONTAIN α3 AND γ1 SUBUNITS AND PRESENT DIFFERENTIAL FUNCTIONAL AND PHARMACOLOGICAL PROPERTIES

by

Rainald Pablo Ordaz, Edith Garay, Agenor Limon, Alberto Pérez-Samartín, María Victoria Sánchez-Gómez, Leticia Robles-Martínez, Abraham Cisneros-Mejorado, Carlos Matute, and Rogelio O. Arellano.

MOLPHARM-AR-2020-000091 - Supplemental Information

Supplementary Figure 1 (S1)

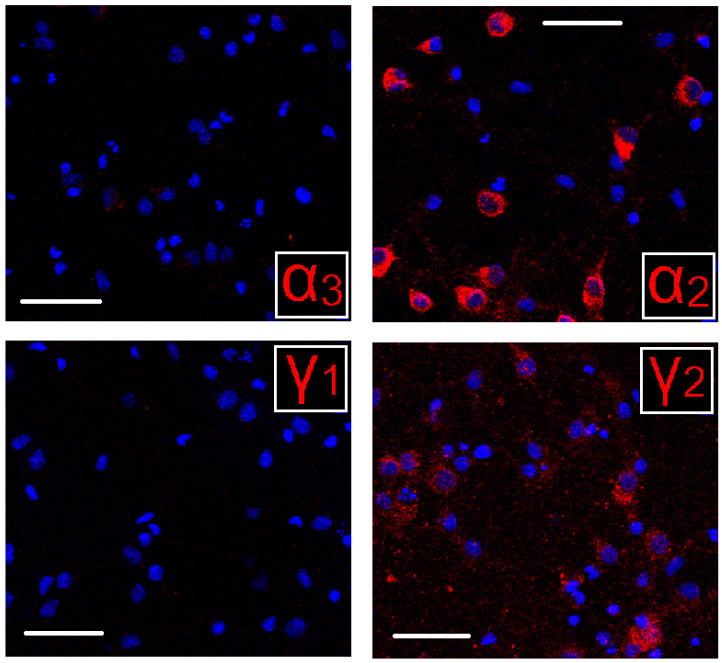

Figure S1. Expression of $GABA_AR$ subunits in cortical neurons. Analysis by immunocytochemistry of rat cortical neurons maintained in culture. Panels show images from confocal microscopy of the fluorescence signal for a specific antibody against the $GABA_AR$ subunit protein (in red) indicated in each panel, and nuclei labeling with DAPI (blue). Bars = 50 μm.

Supplementary Figure 2 (S2)

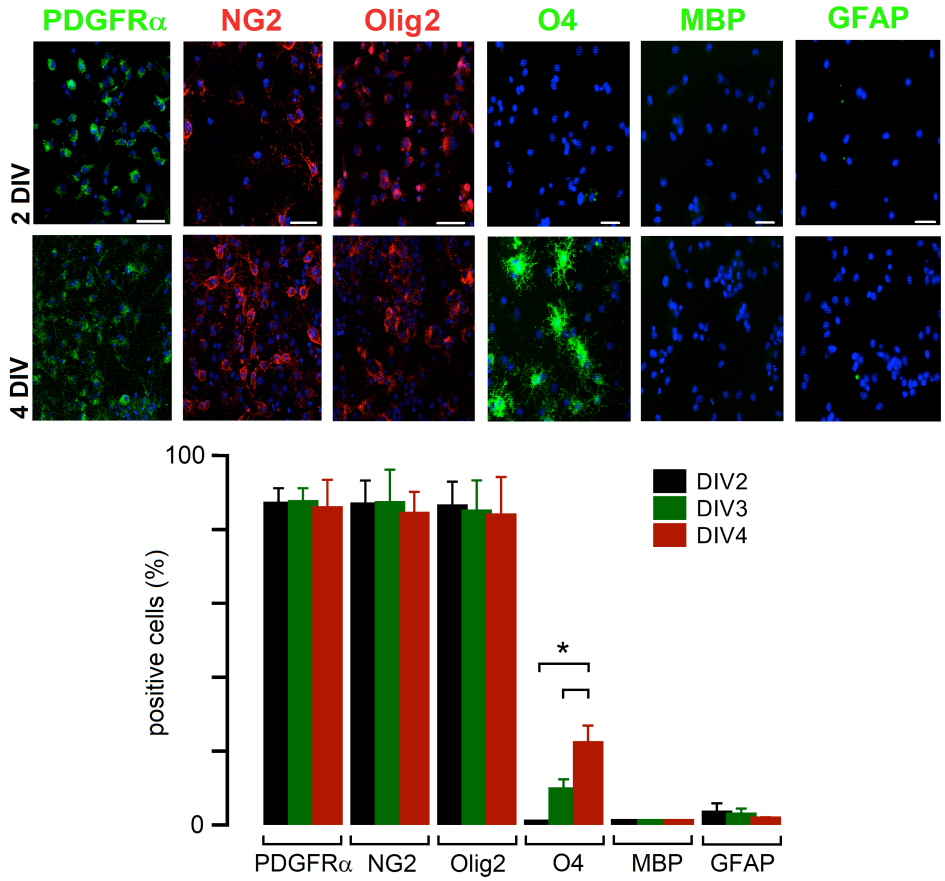

Figure S2. Expression of glial markers in OPCs from 2 DIV to 4 DIV maintained in proliferative medium. Images in the upper panels show representative fields of OPCs maintained in culture and processed for immunocytochemistry at 2 DIV (first row) or 4 DIV (second row). The markers used (indicated at the top) were visualized (either in red or green) by confocal microscopy or epifluorescence. Positive cells for each marker were counted and stated as % of cells (mean ± S.D.) with respect to the total number of cells (nuclei labeled with DAPI) in representative fields. The analysis of expression (% of cells) from 2 DIV to 4 DIV in the column graph indicated that specific markers for OPCs, such as PDGFRα, NG2, and Olig2, maintained expression levels close to 85% throughout the period in culture, while MBP and GFAP, markers for myelinating OLs and astrocytes, respectively, were not detected. Also, O4 showed an increase in its expression that became statistically significant towards 4 DIV. *$p < 0.0001$ 4 DIV compared to 2 DIV and 3 DIV, one-way ANOVA followed by a Tukey's *post hoc* Test.

Supplementary Figure 3 (S3)

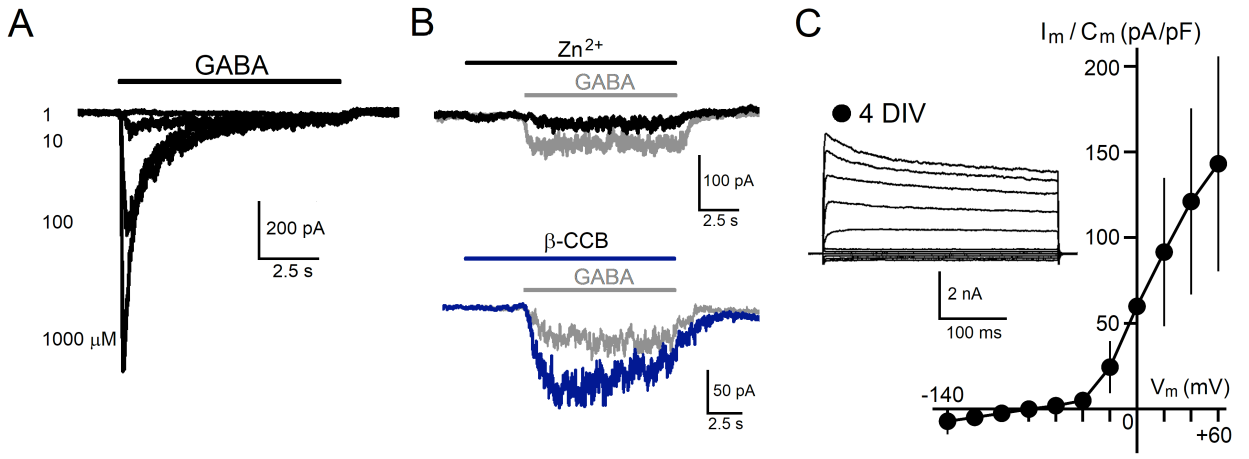

Figure S3. $GABA_AR$ pharmacological profile in OPCs at 4 DIV and their I/V relationship. A) Traces illustrate GABA responses in an OPC at 4 DIV (held at -80 mV) to distinct neurotransmitter concentrations as indicated. D-R curves built with the peak amplitude response in each concentration gave an EC_{50} of 85.2 ± 4.42 µM (n=15 cells). B) Traces illustrate the modulatory effect of either (10 µM) Zn^{2+} or β-CCB on the (10 µM) GABA response. Each set includes the control GABA response in gray and the response in the presence of a modulator (black traces; Zn^{2+} IC_{50} of 20.1 ± 4.24 µM (n=10 cells); β-CCB enhancement of 227.3 ± 59.1% (n=10 cells)). C) OPC I/V relationship at 4 DIV in proliferative medium. Traces illustrate the normalized current membrane response to a voltage-step protocol applied from -140 to +60 mV in cells held at -80 mV. Data points are the normalized (I_m/C_m) peak current (± S.D.) recorded in 30 cells.